Local waveform inversion for source parameters

Peter Suhadolc

Department of Earth Sciences

University of Trieste

ICTP 2004

The questions we would like to address are:

1. How close is the solution of this (unstable) problem to the correct one?

2. How does poor knowledge of crustal structure in the source region affect the estimate of the rupture front location and speed?

3. Since such inversions are non-unique, what methods can one use to choose the "correct" solution from among the multiplicity of solutions?

Since these questions cannot, in fact, be answered when working with real data, we set up a problem using artificial data

Source model

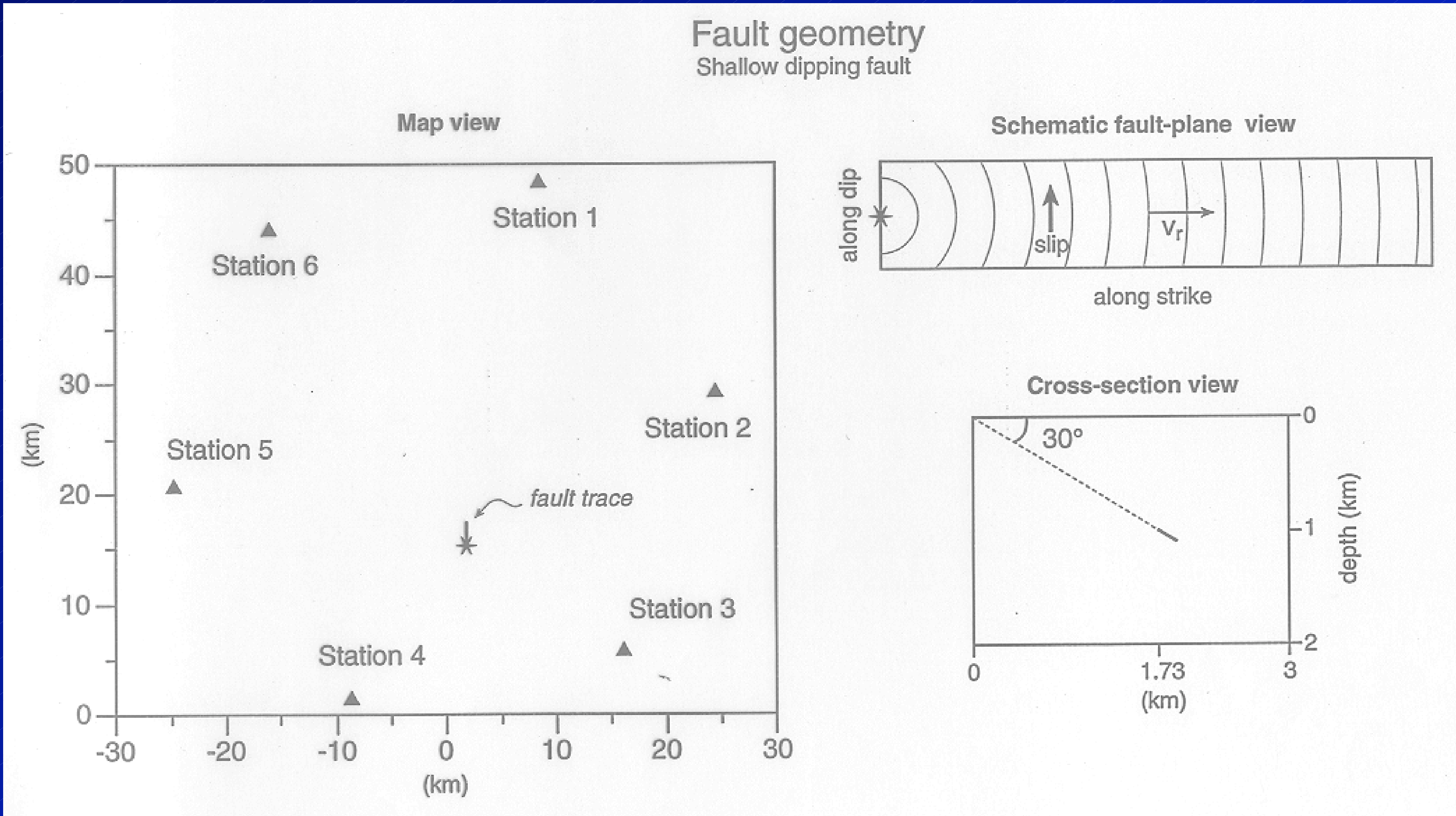

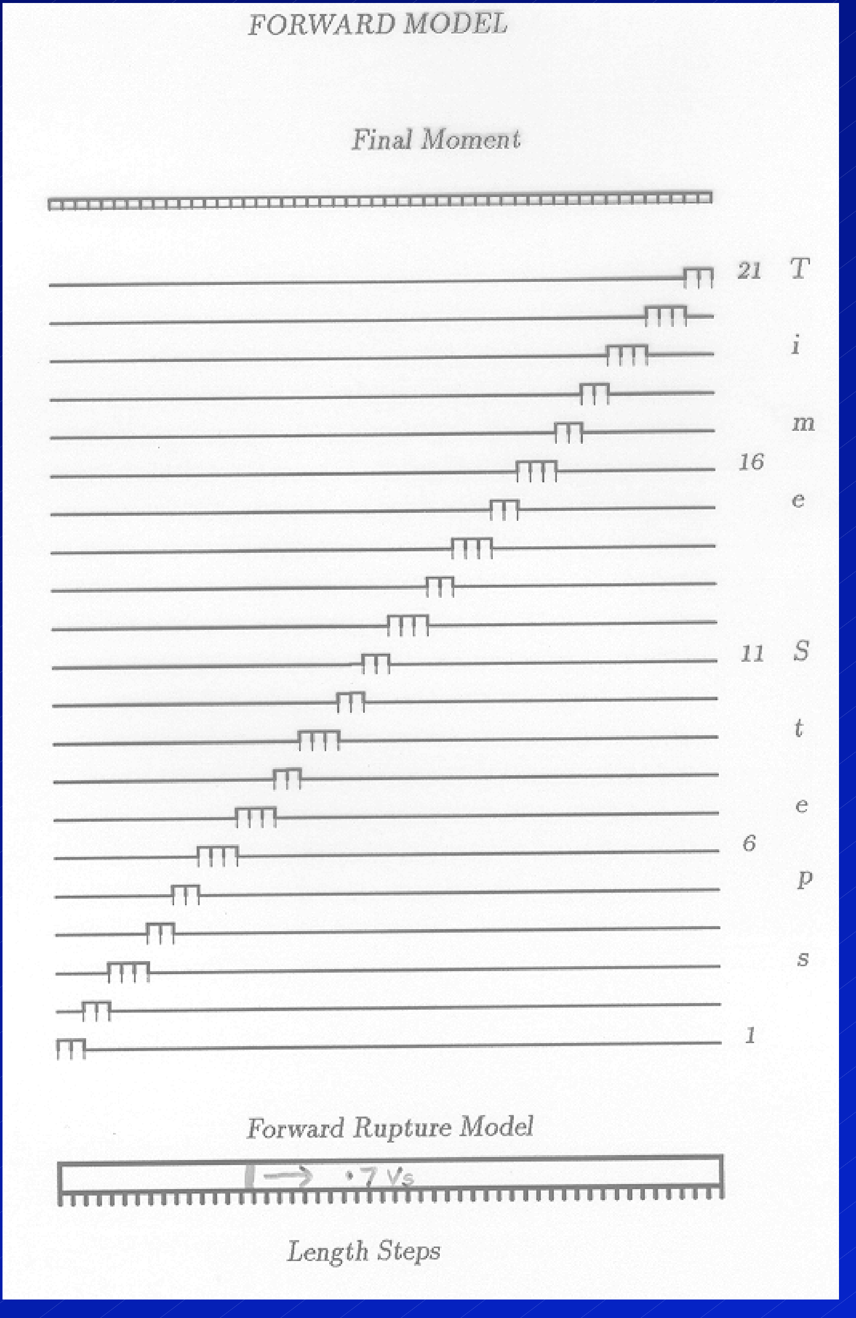

Forward model

1 x 10^{11} Nm of moment are released at each grid, which is allowed to slip **only once**

Rupture speed = 0.7 β

In the first set of cases, the inverse problem is solved using the SAME spatial and temporal grid sizes as those used to generate the synthetic (noise-free) data

Inversion methods

First approach:
SVD, minimize L2 norm
Constrain moment value
Remove small eigenvalues
Solution with smallest first differences

Second approach:
Linear programming, minimize L1 norm
Use different physical constraints
Smallest second differences

Case 1a - conclusions

Even if we constrain the rupture front in the inversion to the true front, we are unable to reproduce the final constant moment distribution and the source time function, when we use the SVD method: many small, negative values of moment rates are produced

Case 1b - conclusions

When we constrain the moment rates to be POSITIVE (using the linear programming method) we are able to reproduce the final constant moment distribution and the source time function correctly!

Case 1c - conclusions

When we constrain the rupture front to move **faster** than the true one and also allow all cells behind it to continue to slip, we are able to reproduce the solution (moment-rate history, final moment, source time function) as long a sthe **POSITIVITY** constraint is used

Case 1c

Rupture front

Forward model = 0.7 β

Inverse model = 0.5 β

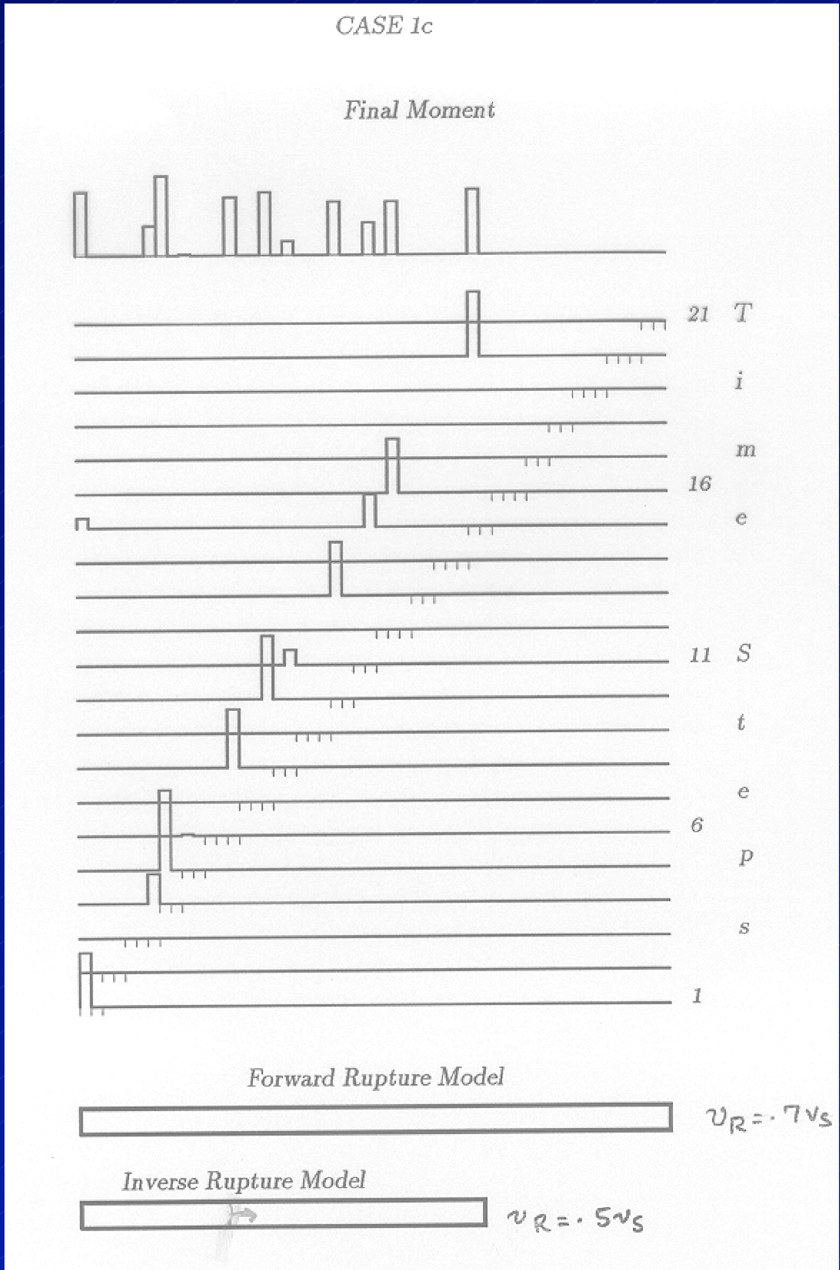

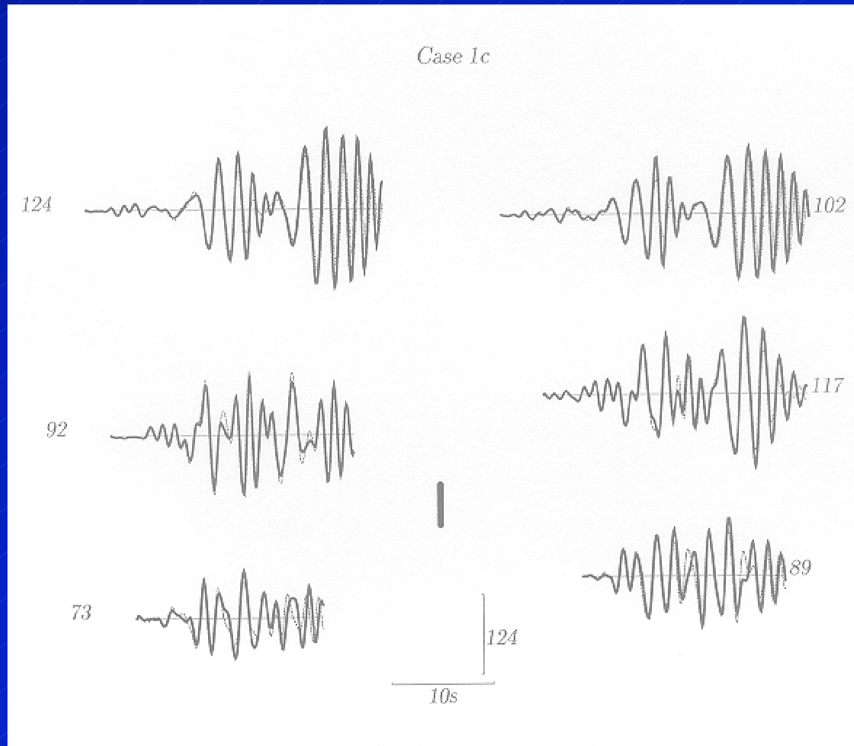

Case 1c - conclusions

If the rupture front is constrained to move **more slowly** then the true one, we are unable to reproduce any aspect of the solution correctly, **even with the positivity constraint**. Constraining the seismic moment to the true one does not improve the solution.

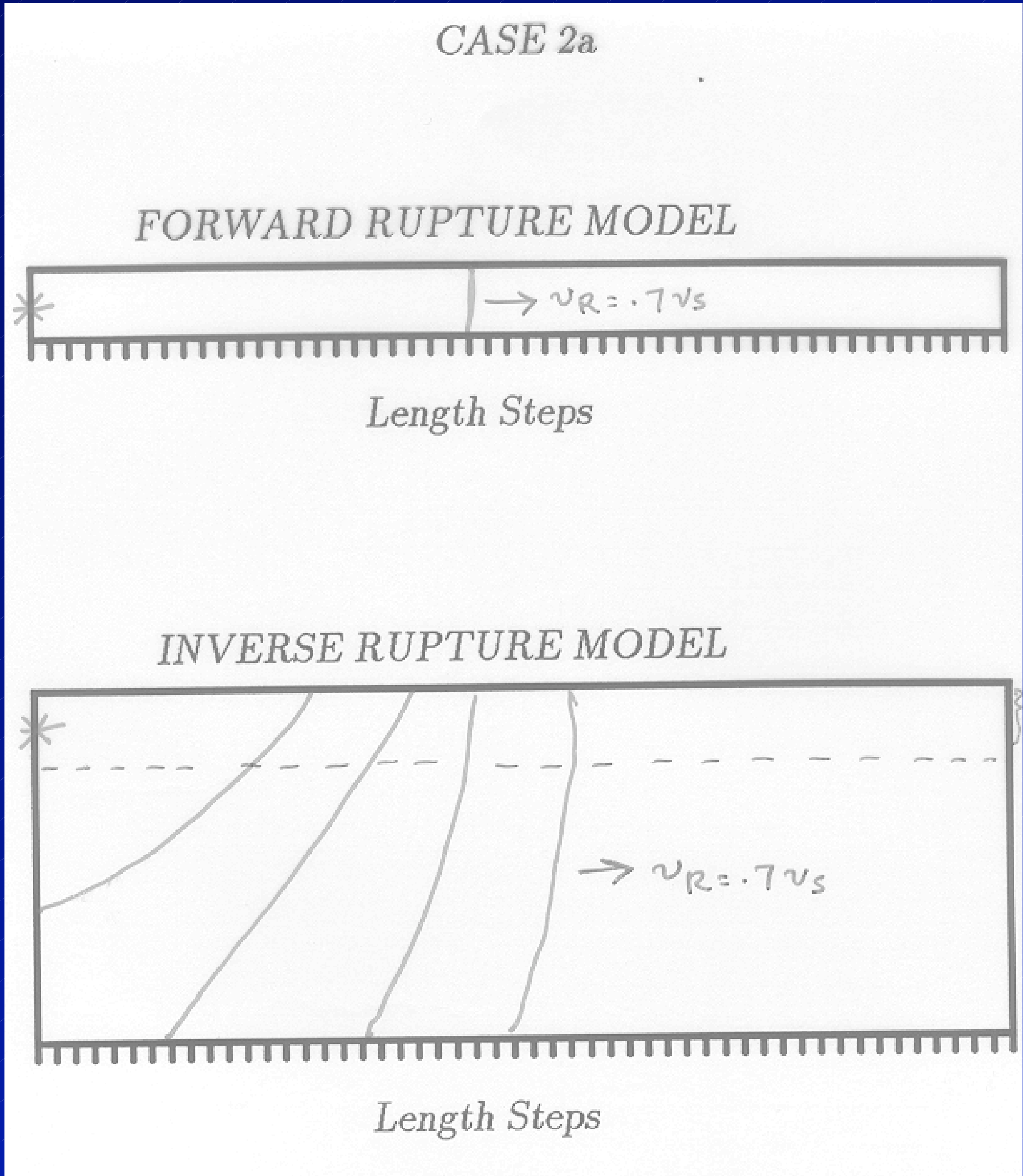

Case 2a
Wider fault

Same rupture speed in forward and inverse model
0.7 β

Case 2a - conclusions

If we use a wider fault and the correct rupture speed and allow cells to release moment only once in the inversion, and also impose the positivity constraint, then the moment is only released at the correct depth in the solution, even though moment release at deeper parts of the fault was permitted

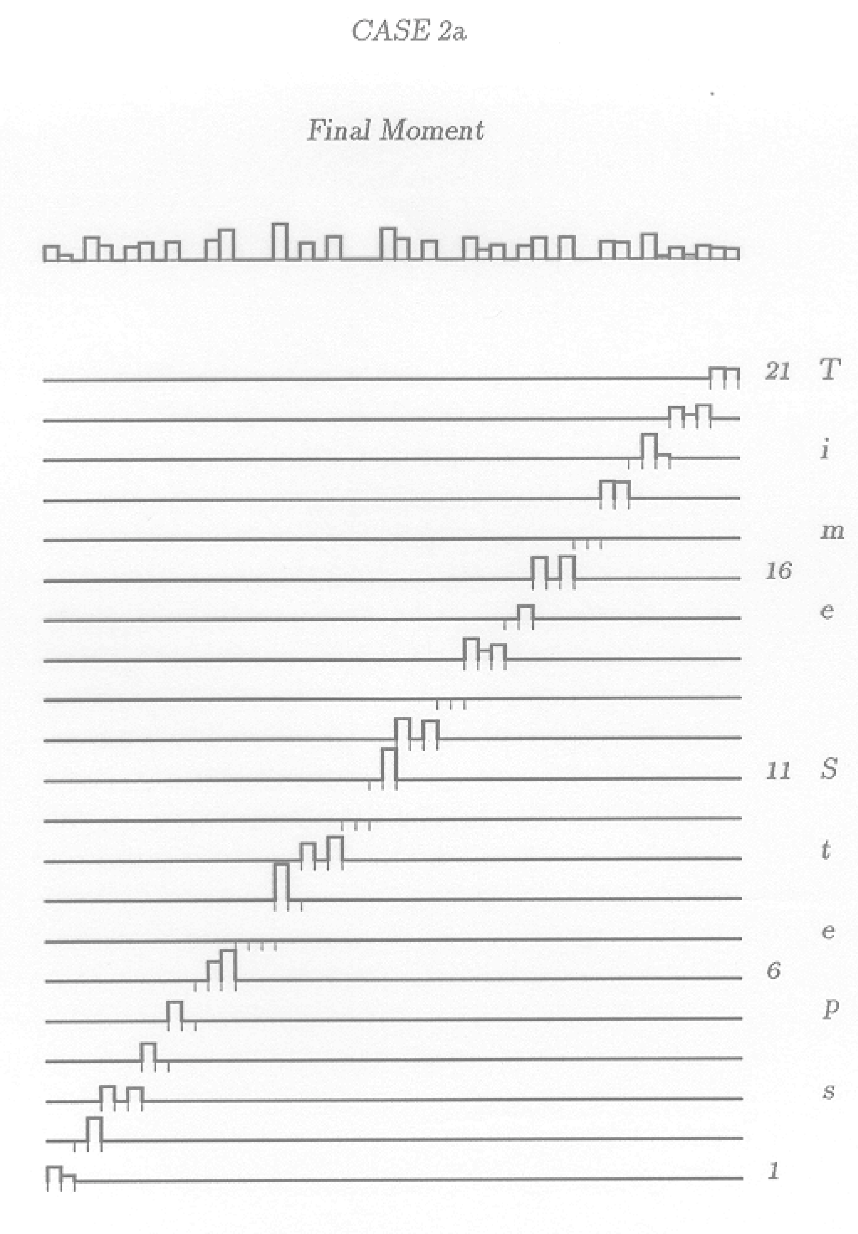

Case 2a
Wider fault

Inversion results

The constant moment release is reproduced approximately

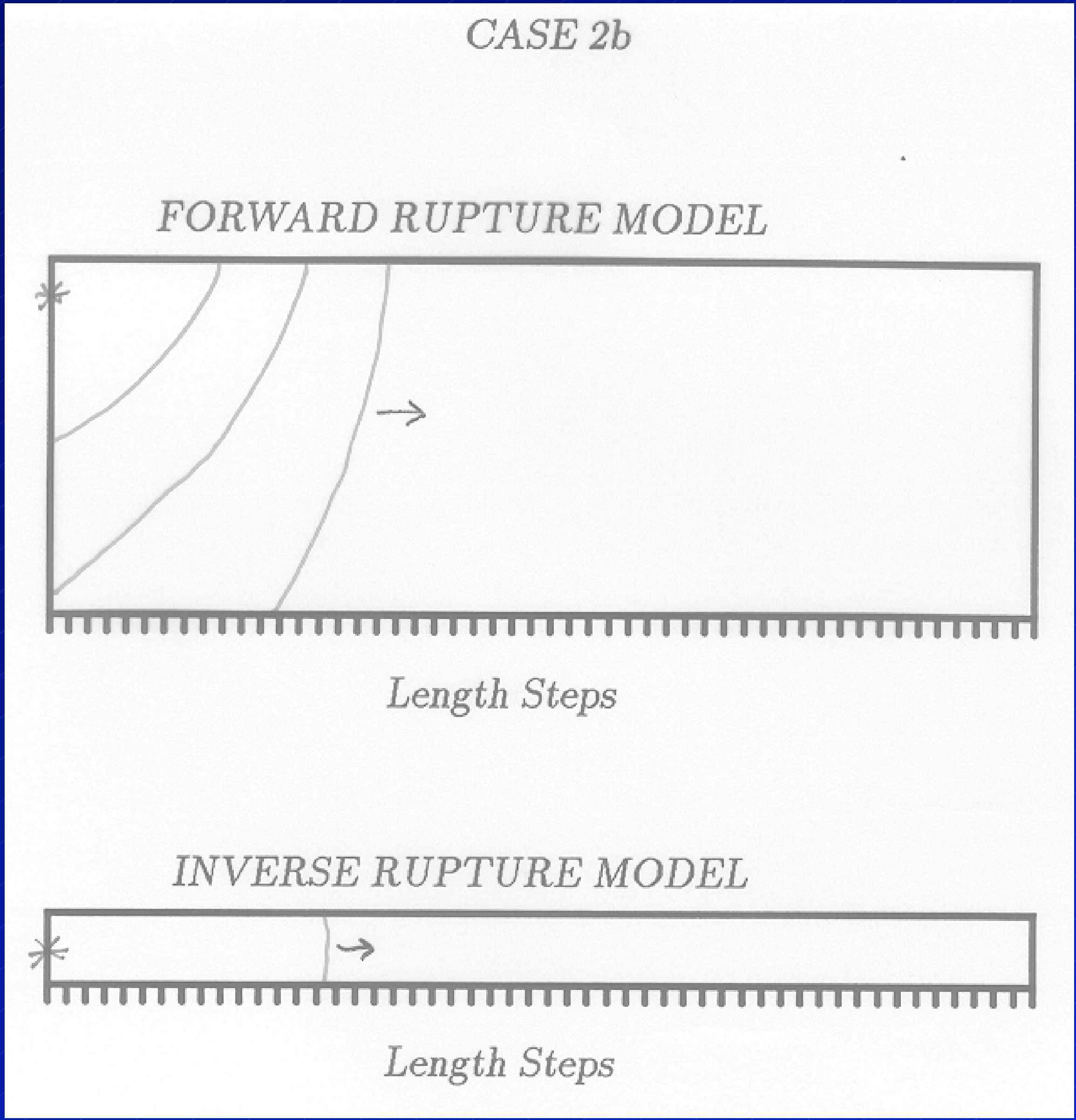

Case 2b
Narrower fault

Same rupture speed 0.7 β

Case 2b - conclusions

If we use a narrower fault than the true one in the inversion, we obtain the correct moment and centroids, but are unable to reproduce the source time function and the uniform moment release at the rupture front

But we are able to fit the data!

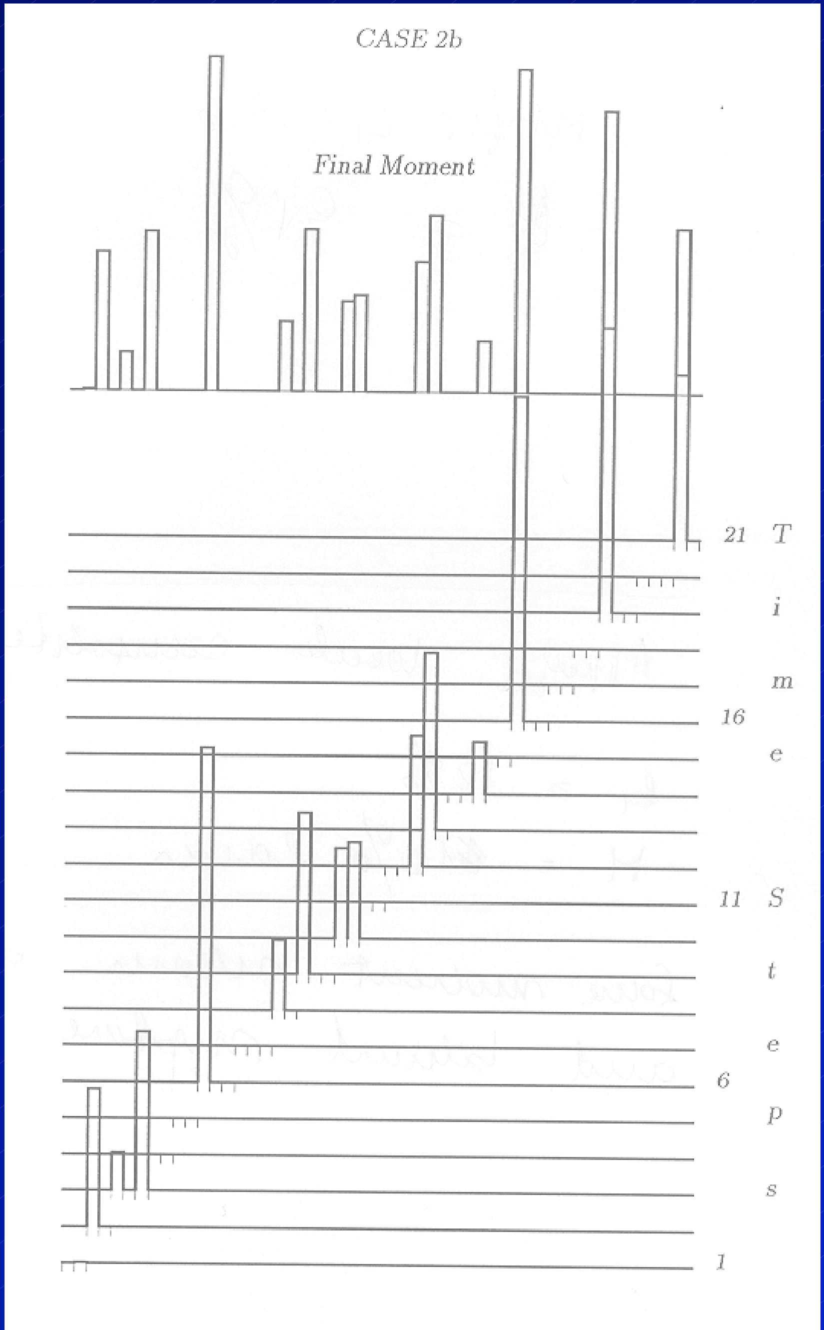

Case 2b
Narrower fault

Strongly non-uniform moment distribution (asperities!)

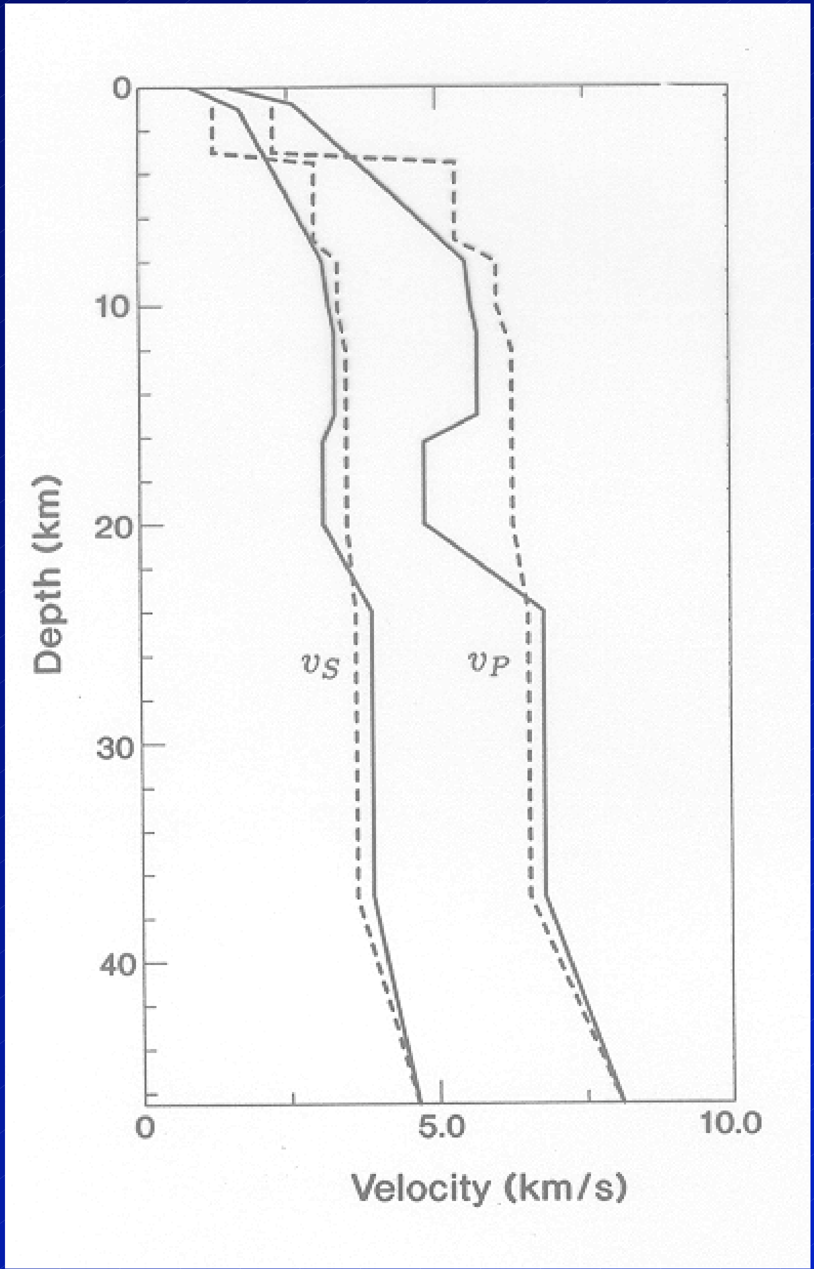

Case 3a

Different medium used in forward (M1, continuous) and inverse model (M2, dashed)

Case 3a
Different medium

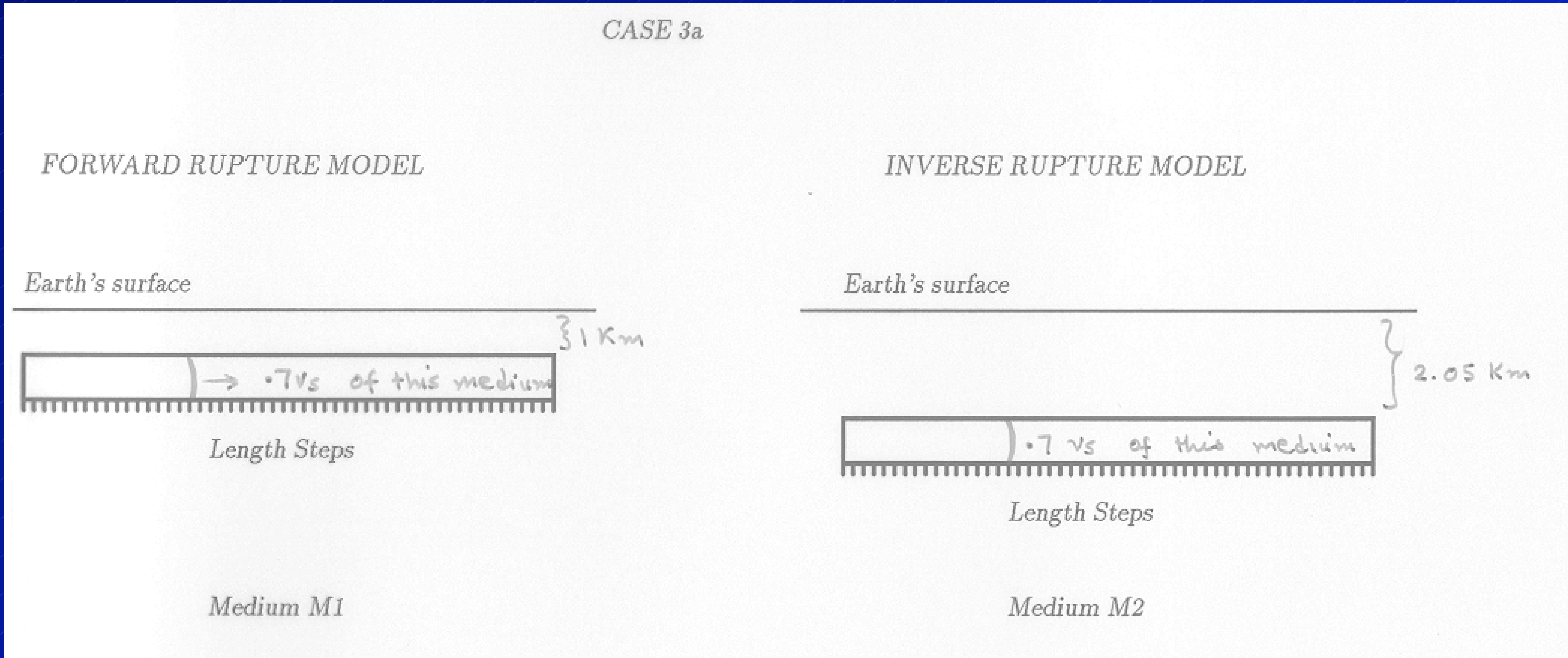

Case 3a - conclusions

Incorrect source structure leads to poor fitting of the data and the solution is not reproduced.
Instead, this incorrect source structure is transformed into ARTIFACTS of the solution!

An illustration of the effect of model noise

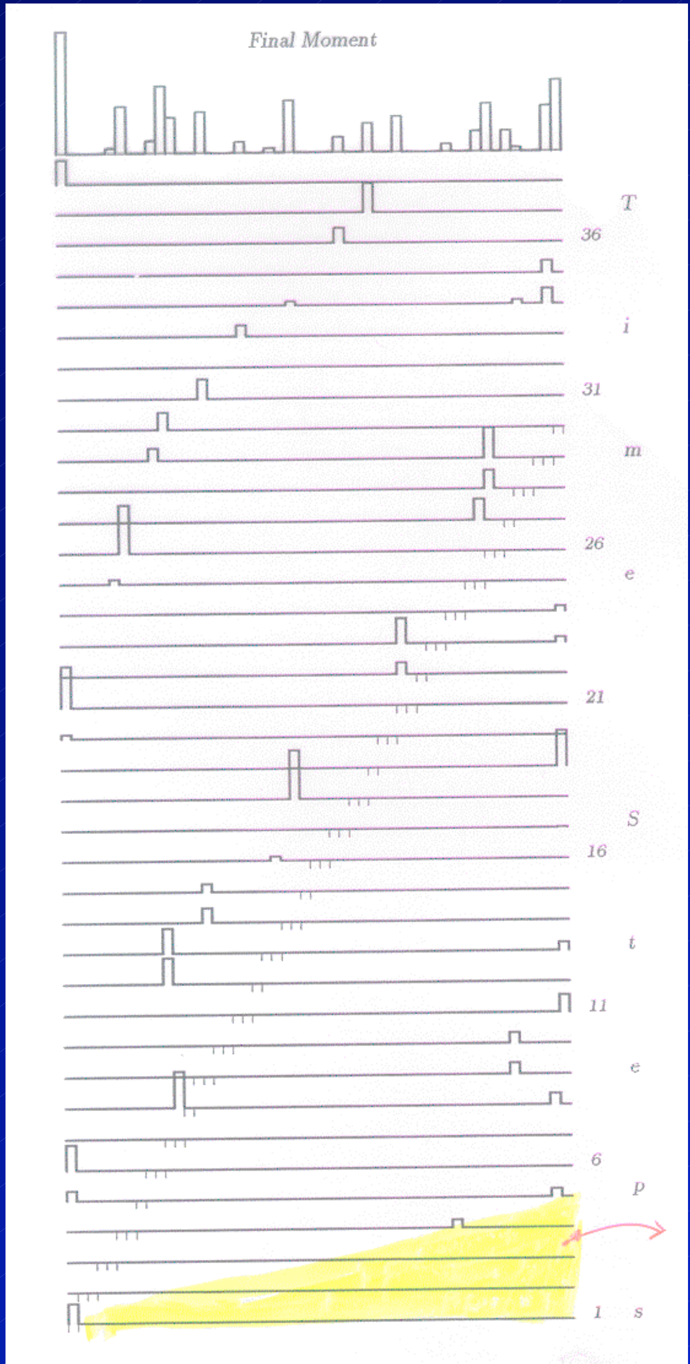

Case 3a

Incorrect source structure

Appearance of artifacts: a GHOST front Behind the main rupture front

Region excluded by weak causality constraint

CONCLUSIONS

In summary, if the Earth structure is known, then we can determine the rupture front location in time, as long as we use a larger fault area and larger rupture speed than the true ones.

CONCLUSIONS

All our negative conclusions, say the fact that we are unable to reproduce the correct solution without the positivity constrant, will hold for more complex cases

CONCLUSIONS

On the other hand, our positive conclusions, say the cases when we can reproduce the rupture front position correctly by using the positivity constraint, is only applicable to the simple forward model studied here

CONCLUSIONS

Larger faults (20 km x 5 km), top of the fault located at 5 km depth. We use 8 times larger spatial and 4 times larger temporal steps in the inversion. Positivity of moment rate enforced. Results compared with forward model smoothed over the larger grids. Similar conslusions as before.

CONCLUSIONS

This study demonstrates the problems we encounter even for the simple case of a Haskell-type faulting model. Clearly more realistic models, like crack models, and models with larger variability of rupture propagation speeds would present even greater difficulties.

Slide

Fault geometry

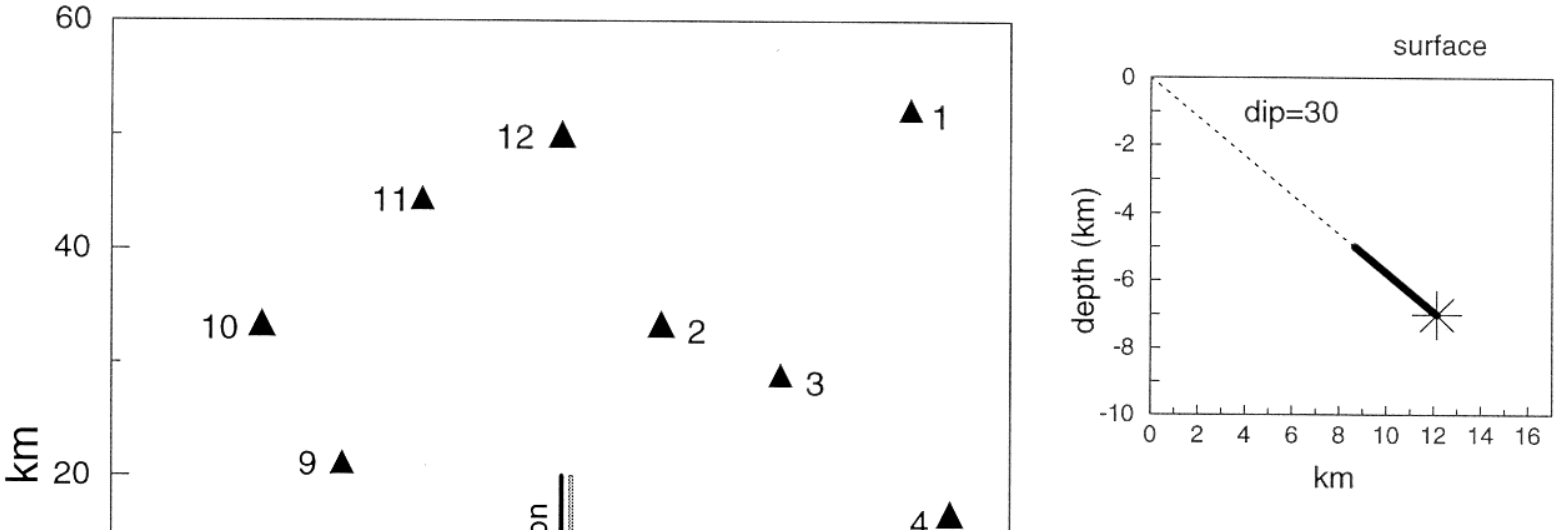

rupturing model

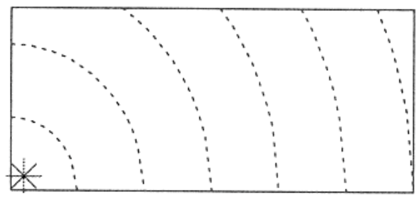

rupturing speed = .7vs

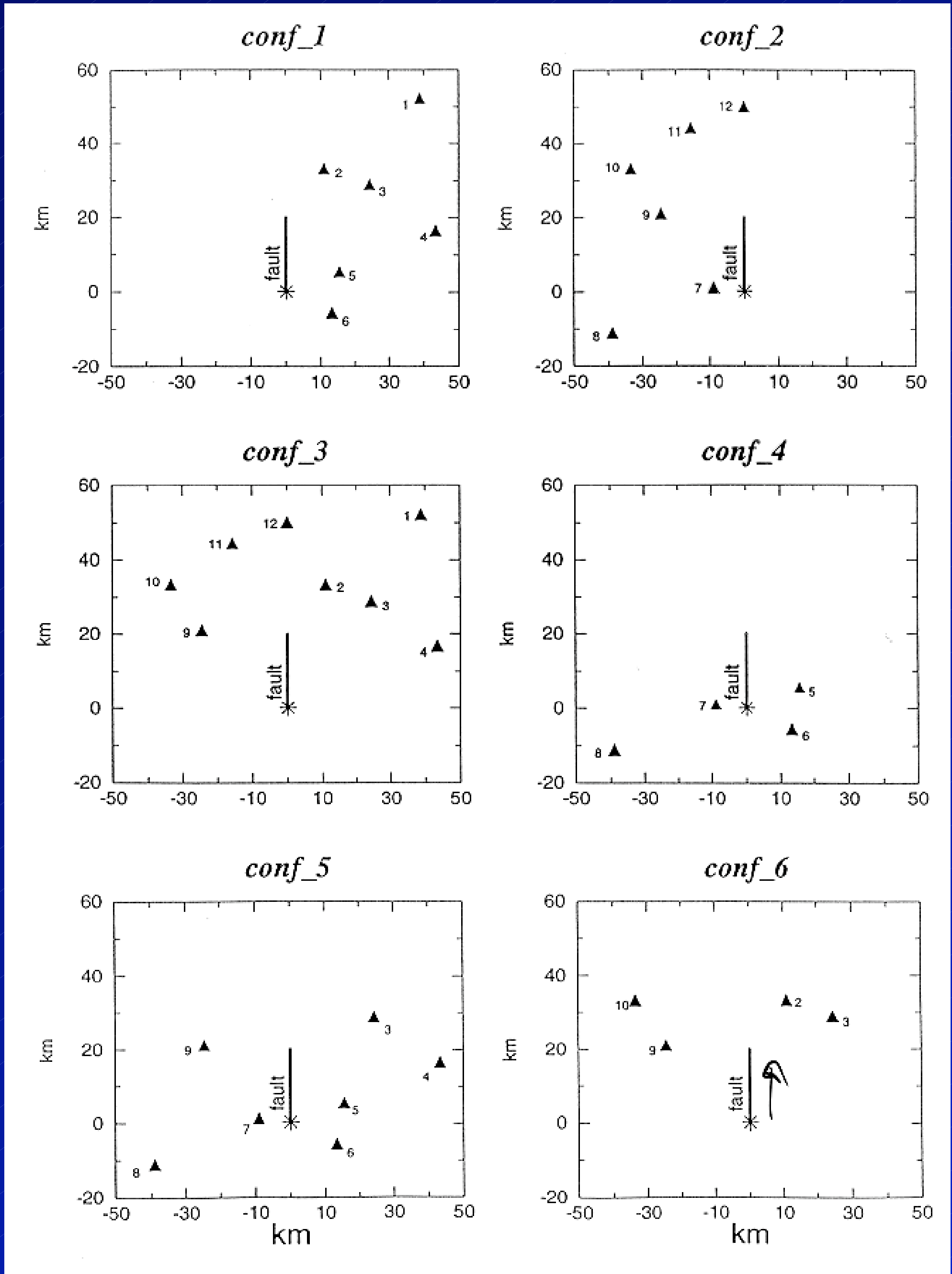

ICTP 2004

Conf_1:
Stations on the hanging wall
Conf_2:
Stations on the footwall
Conf_3 & 6:
Stations in the forward rupture propagation direction
Conf_4 & 5:
Stations in the backward rupture propagation

CONCLUSIONS

A distribution of stations on the hanging wall and in the forward rupture propagation direction allows the source model to be retrieved even in the presence of a small number of stations.

A good azimuthal distribution is more important than the number of stations!

Inversion of the

Bovec 1998 (W Slovenia)

event

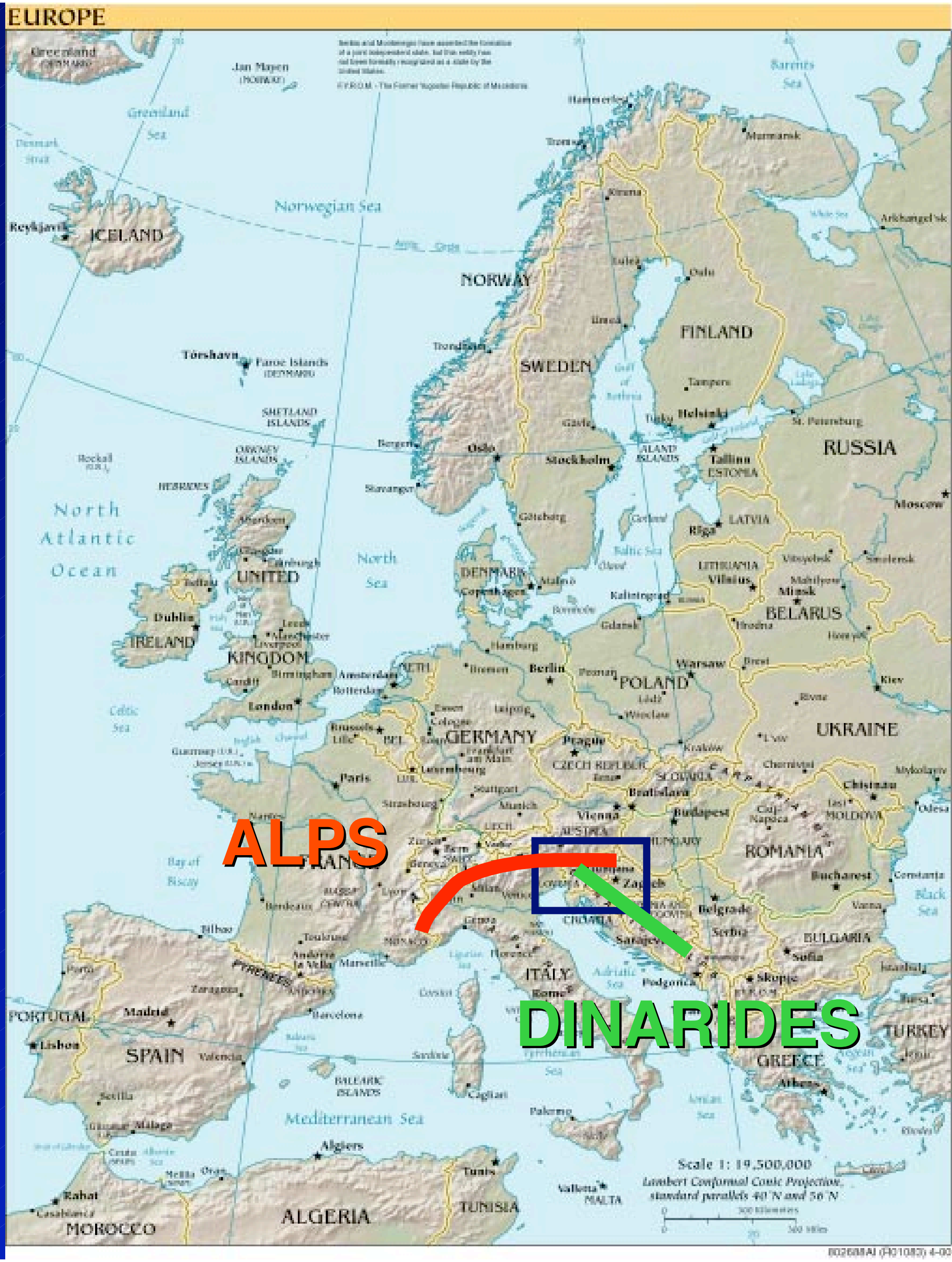
EUROPE
ALPS
DINARIDES
ICELAND
NORWAY
SWEDEN
FINLAND
RUSSIA
UNITED KINGDOM
IRELAND
GERMANY
POLAND
UKRAINE
BELARUS
ROMANIA
SPAIN
PORTUGAL
ITALY
GREECE
TURKEY
BULGARIA
ALGERIA
MOROCCO
TUNISIA
North Atlantic Ocean
Norwegian Sea
North Sea
Mediterranean Sea
Scale 1: 19,500,000

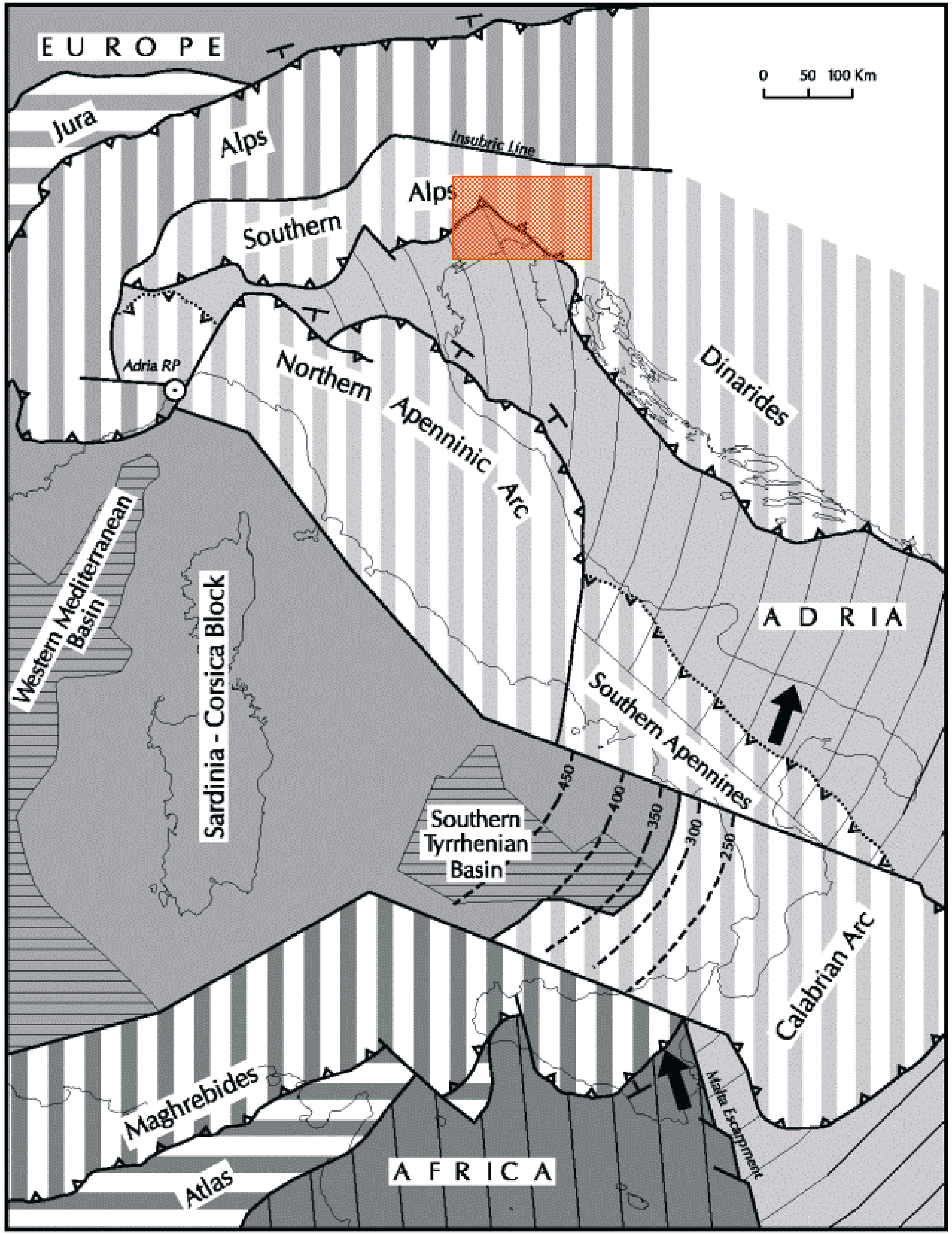

Geodynamic Framework

Historical seismicity

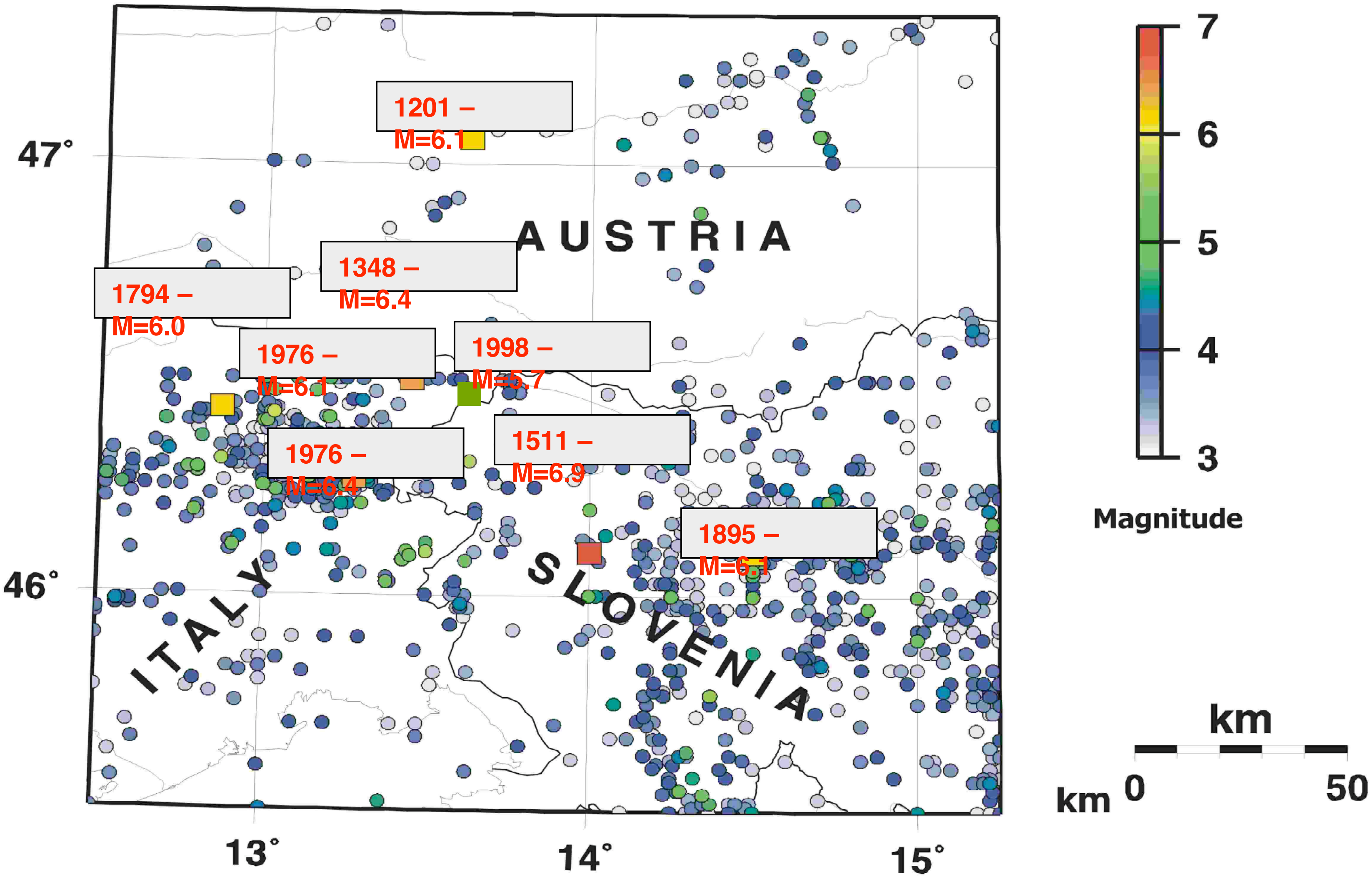

Active deformation and recent seismicity

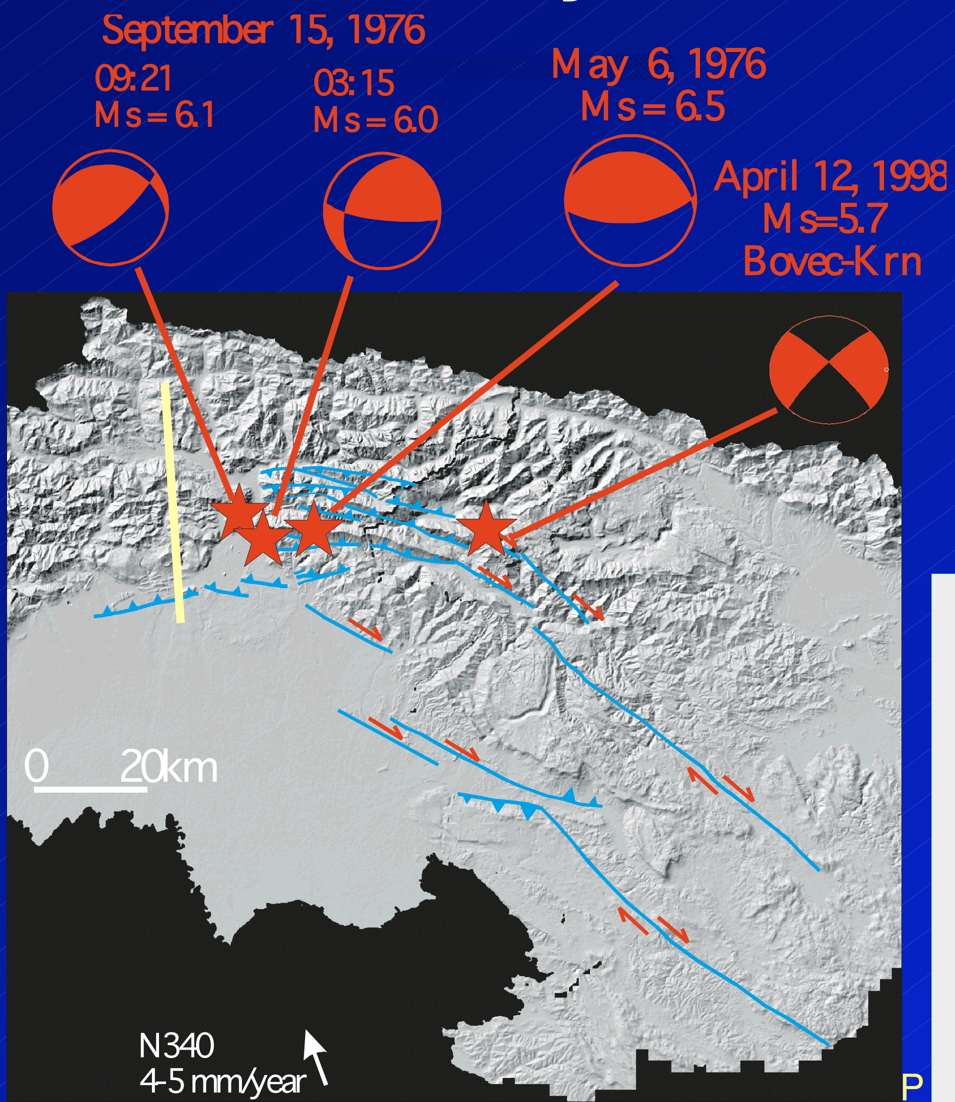

Microseismicity 1977-1987 (Renner, 1995)

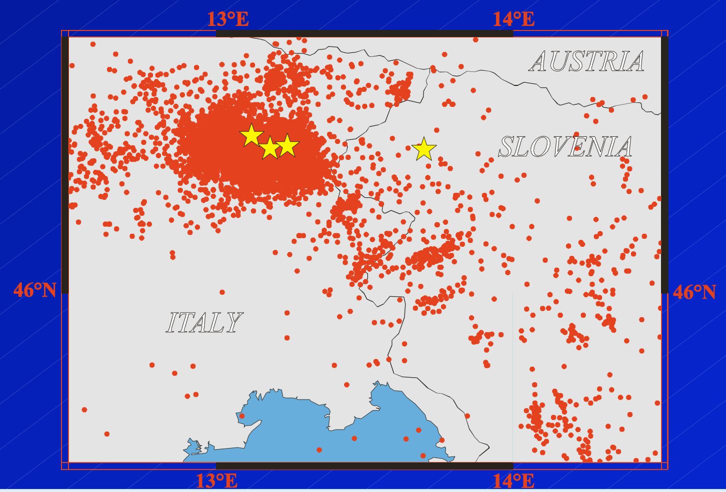

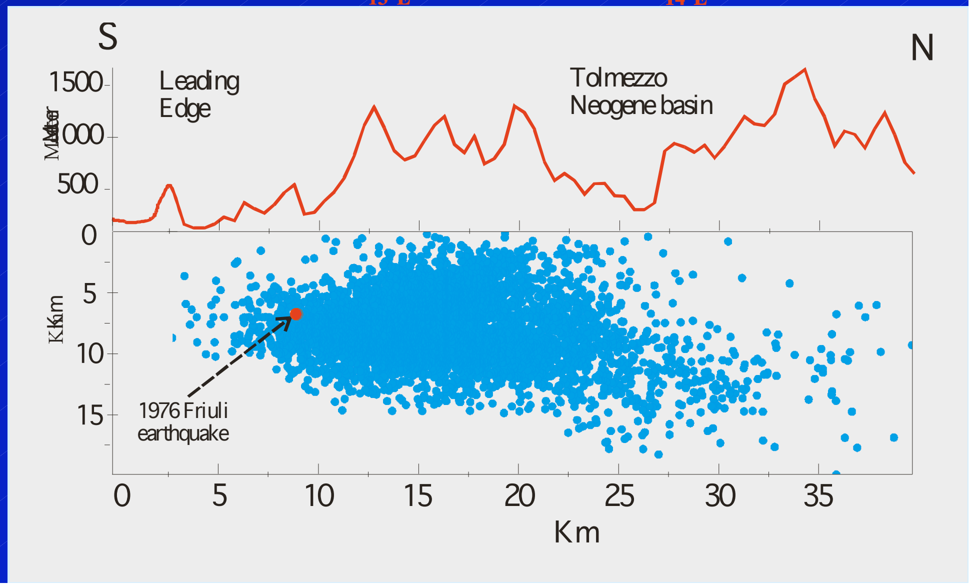

The 1976 Friuli thrust fault and related earthquake sequence

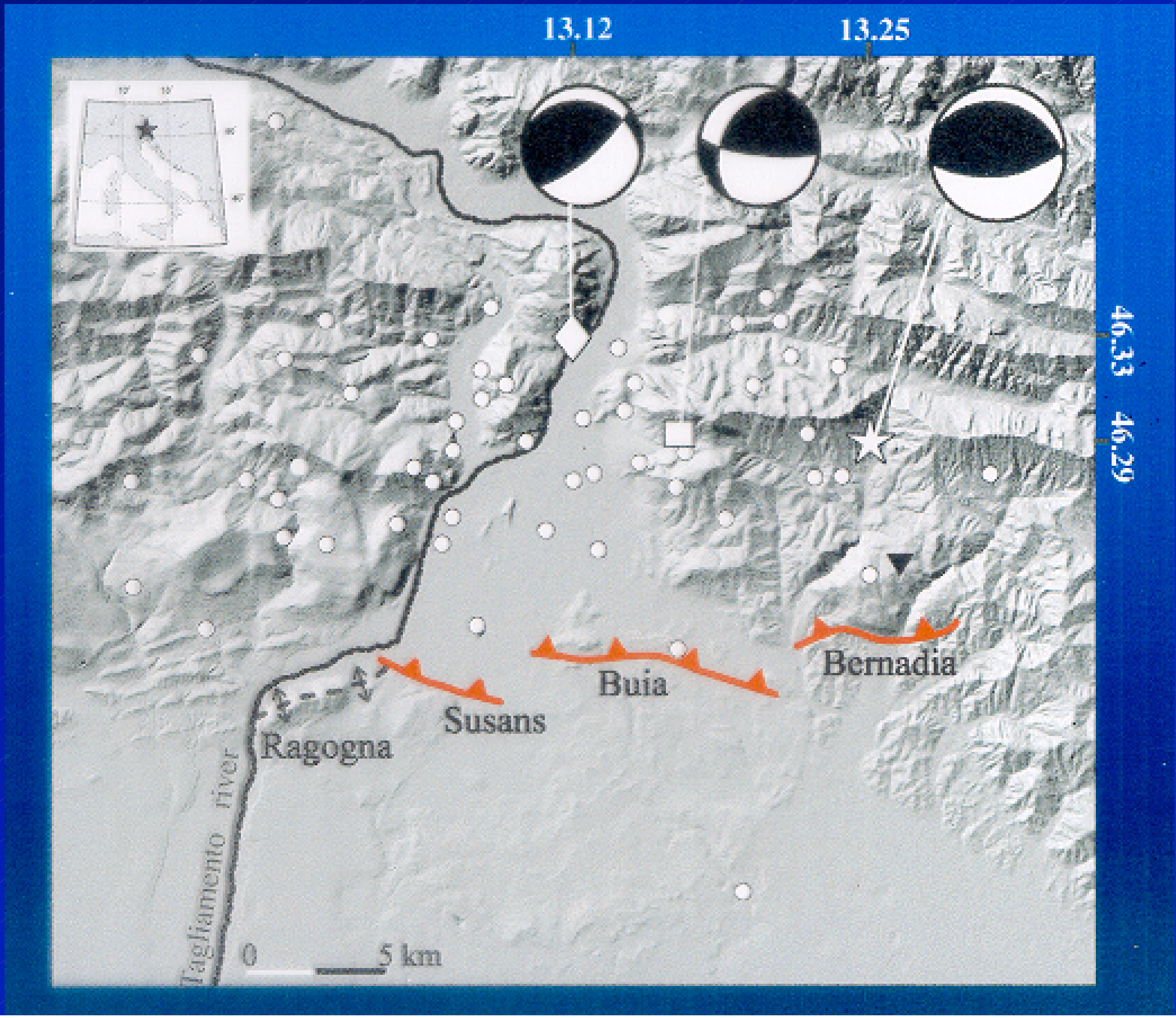

The 1976 Friuli Thrust-faulting Earthquake, Ms 6.5

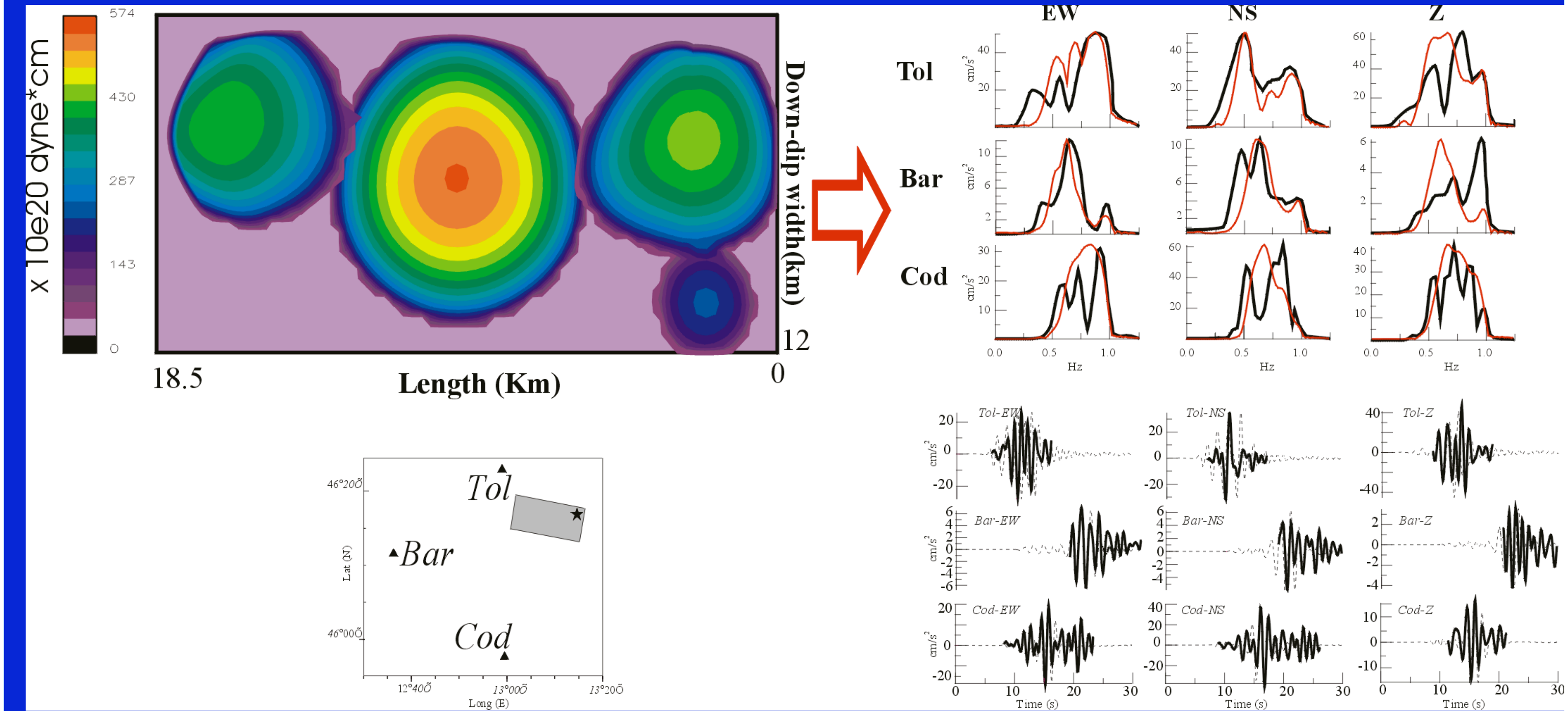

The Bovec-Krn (Slovenia) April 12, 1998 event

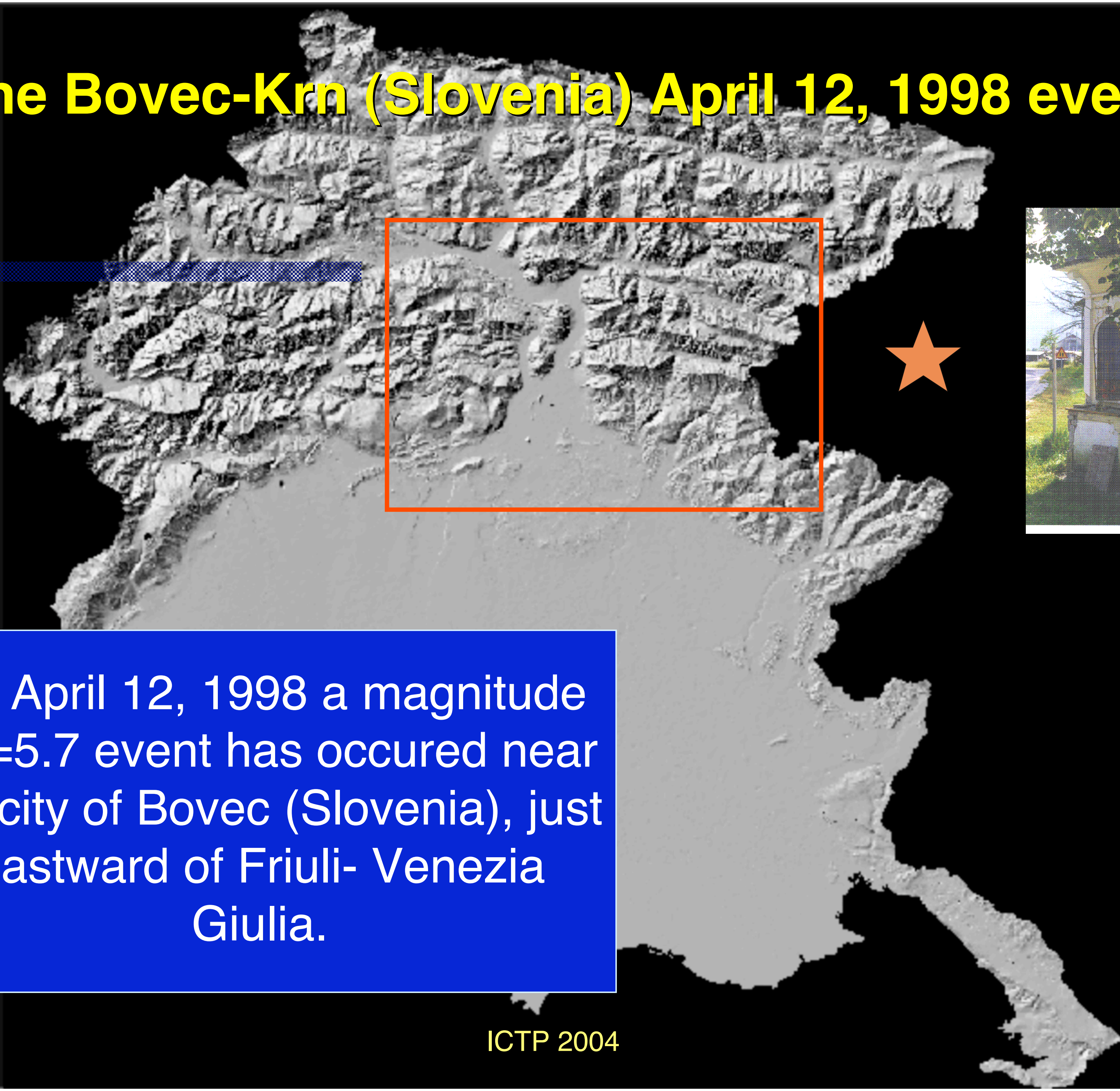

On April 12, 1998 a magnitude Ms=5.7 event has occured near the city of Bovec (Slovenia), just eastward of Friuli- Venezia Giulia.

The 1998 Bovec-Krn Strike-Slip Earthquake, Ms 5.7

Observed Intensities (EMS-98)

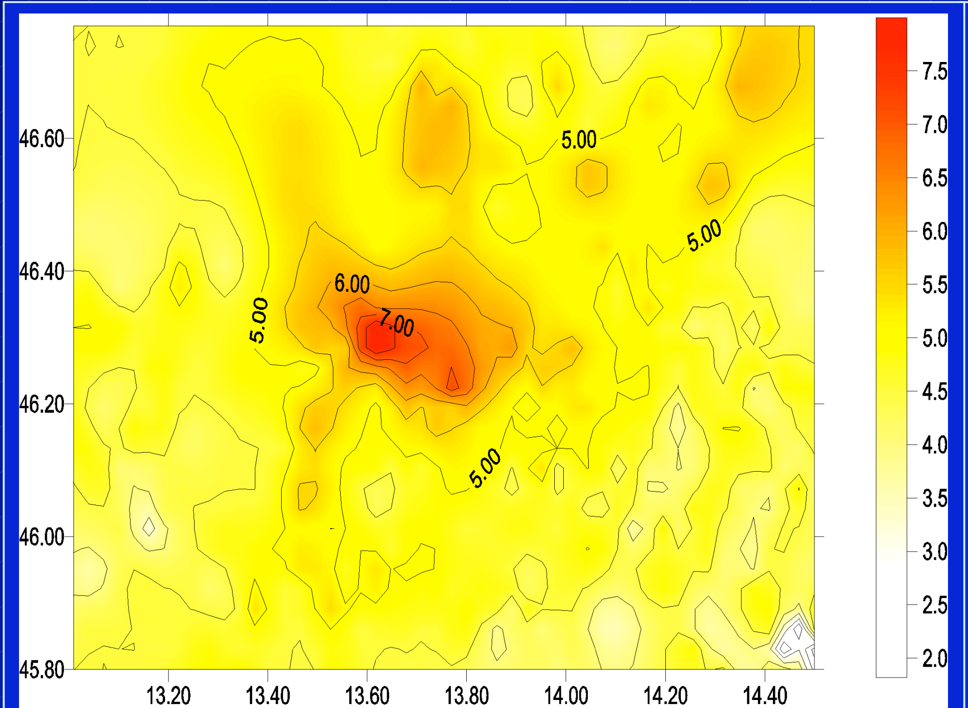

Maximum Horizontal Velocities (cm/s)

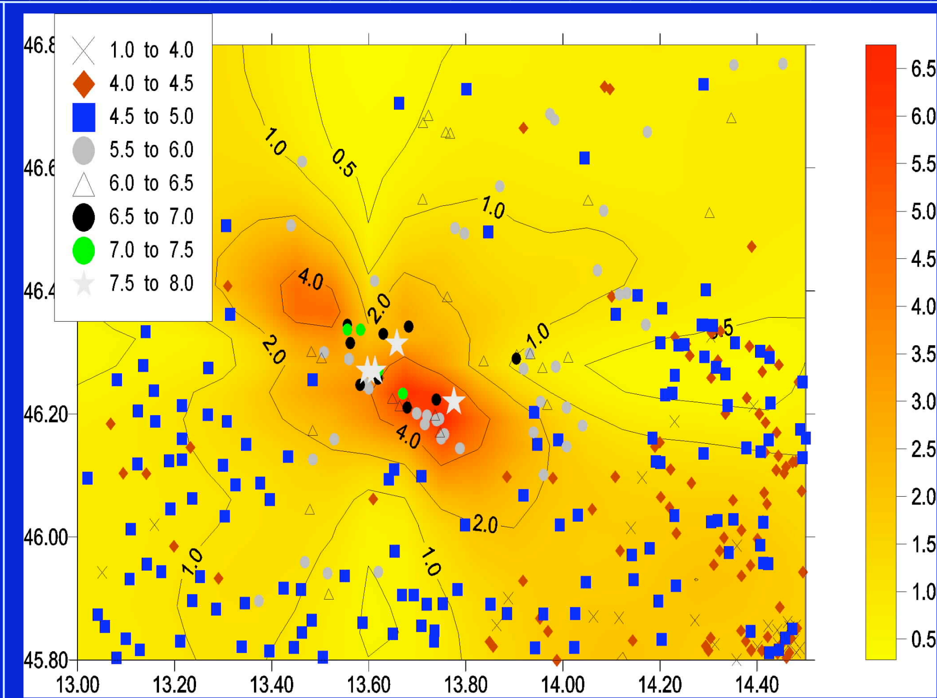

Bovec 1998 - Locations

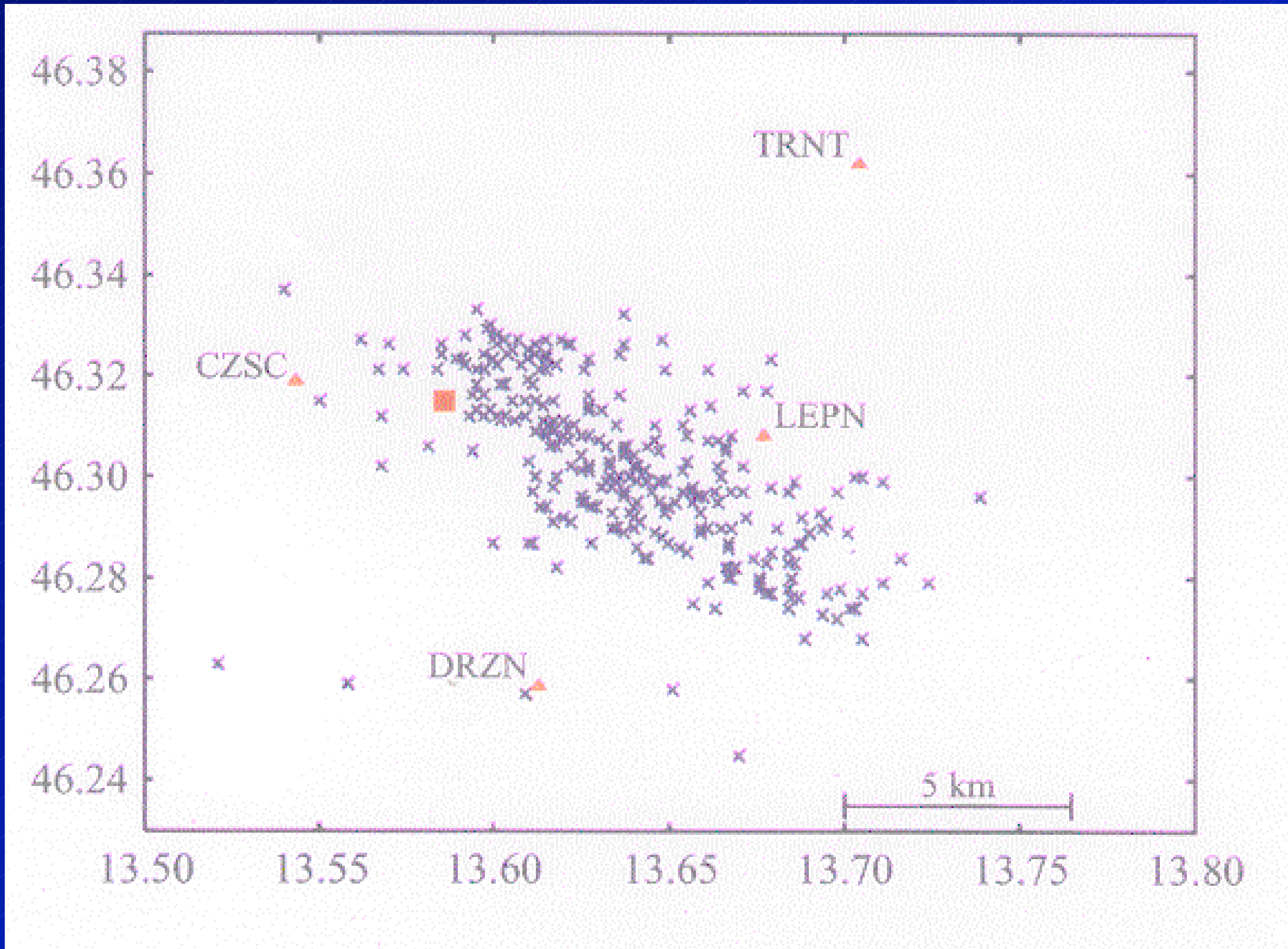

Bovec 1998 - Relocations

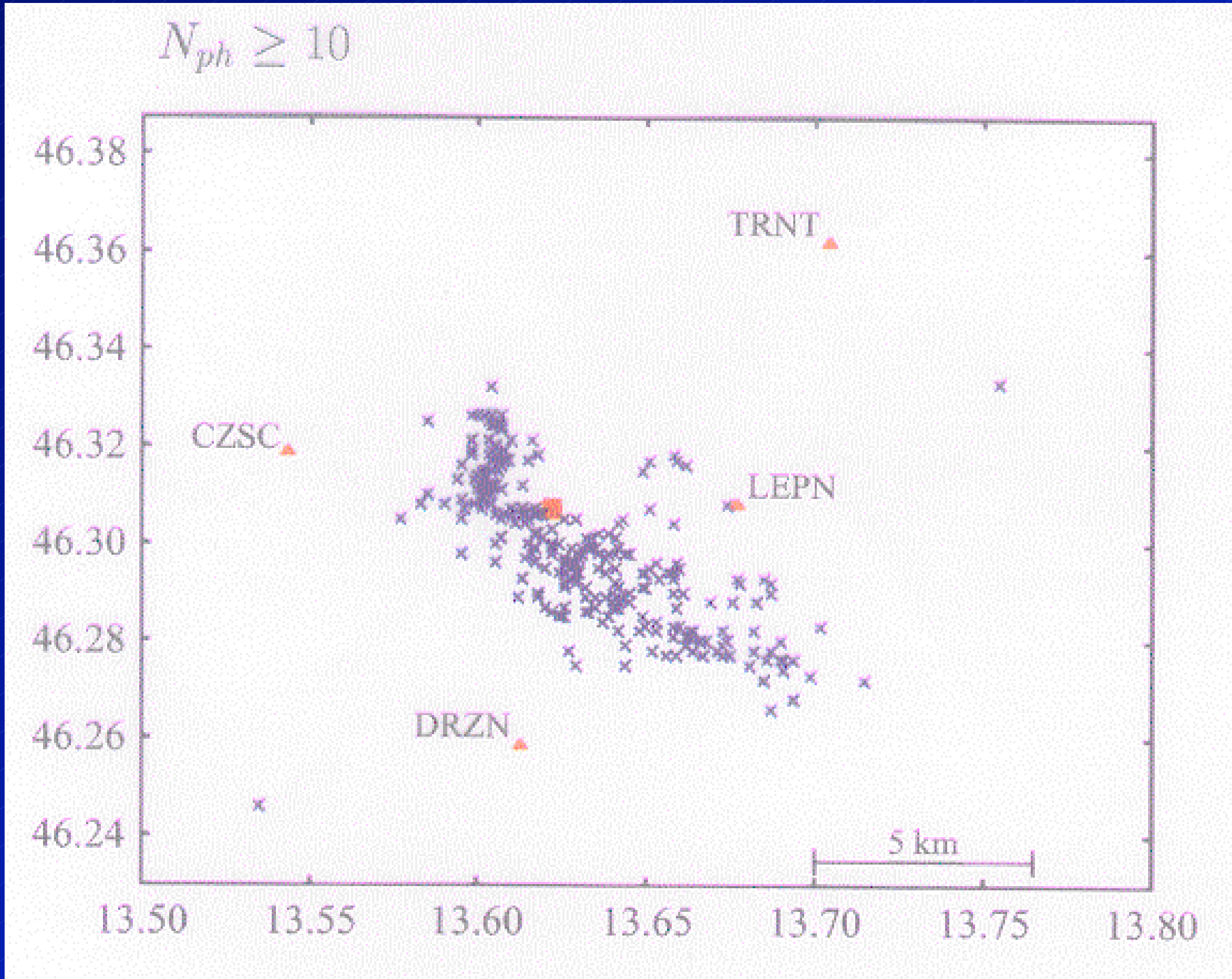

Bovec 1998 - Relocation errors

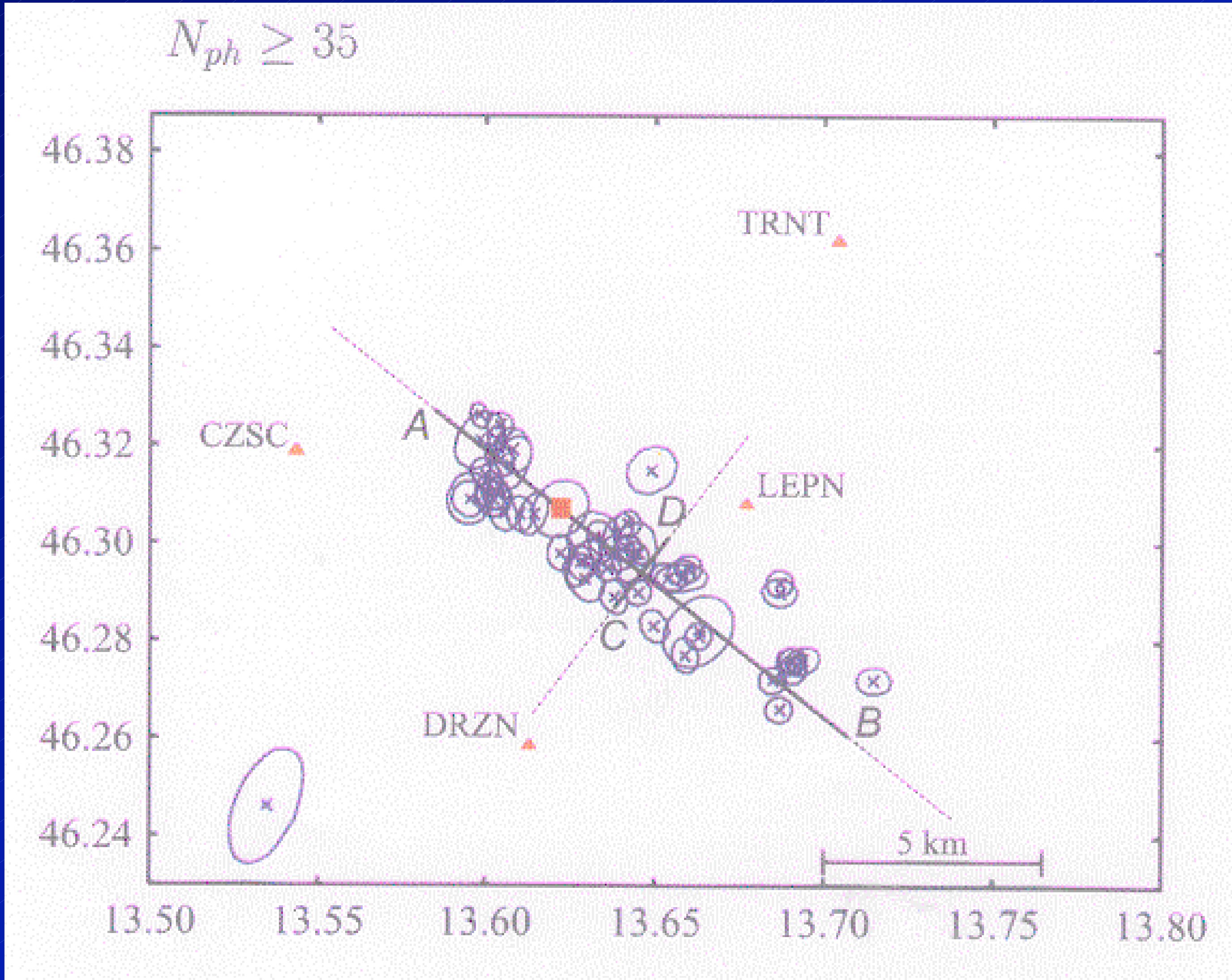

The 1998 Bovec earthquake seque

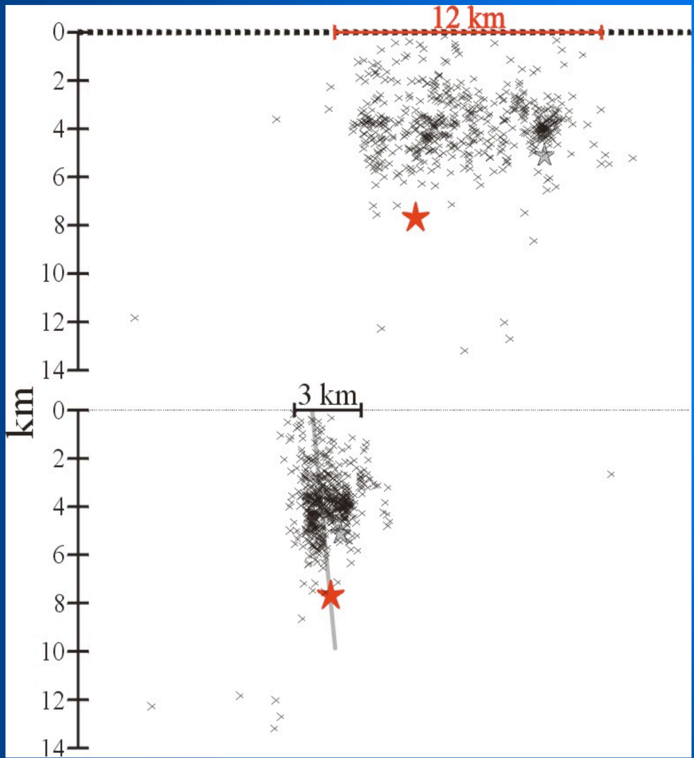

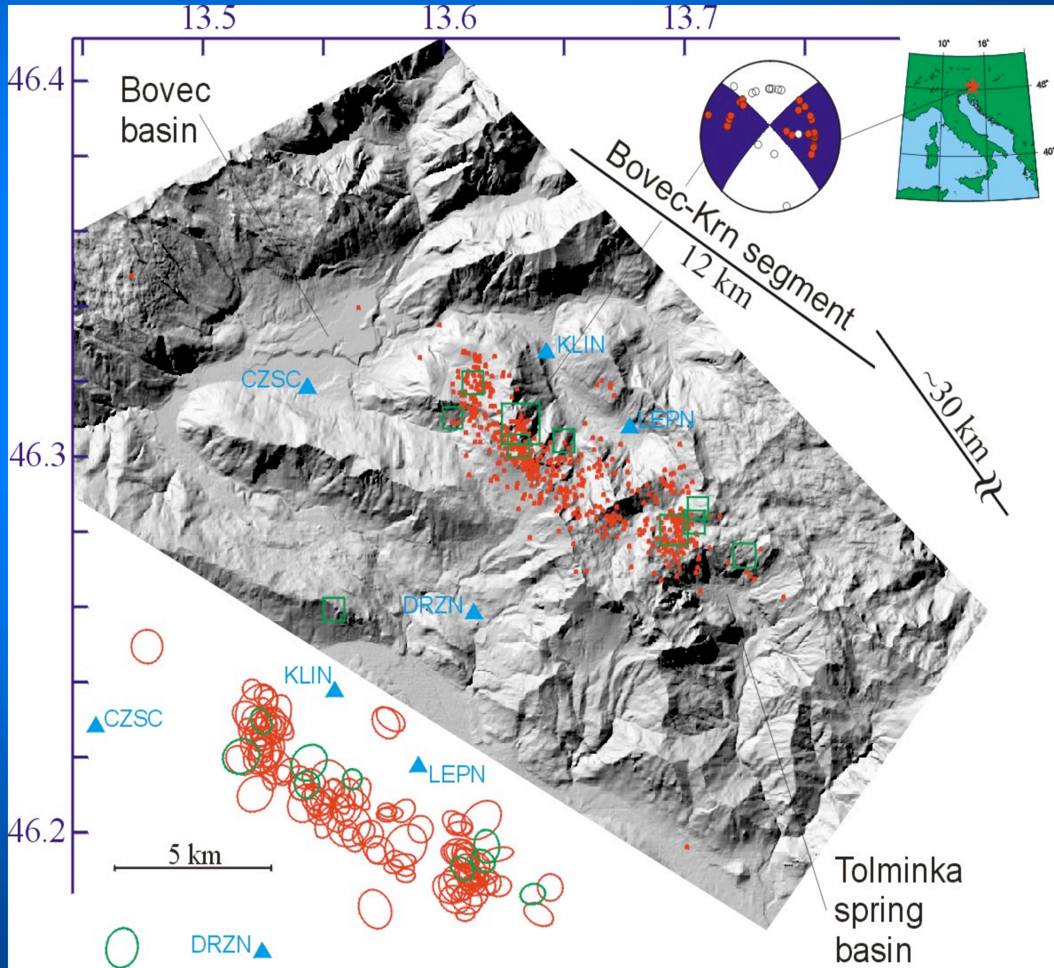

ICTP 2004

Filtering of data - max freq 1 Hz

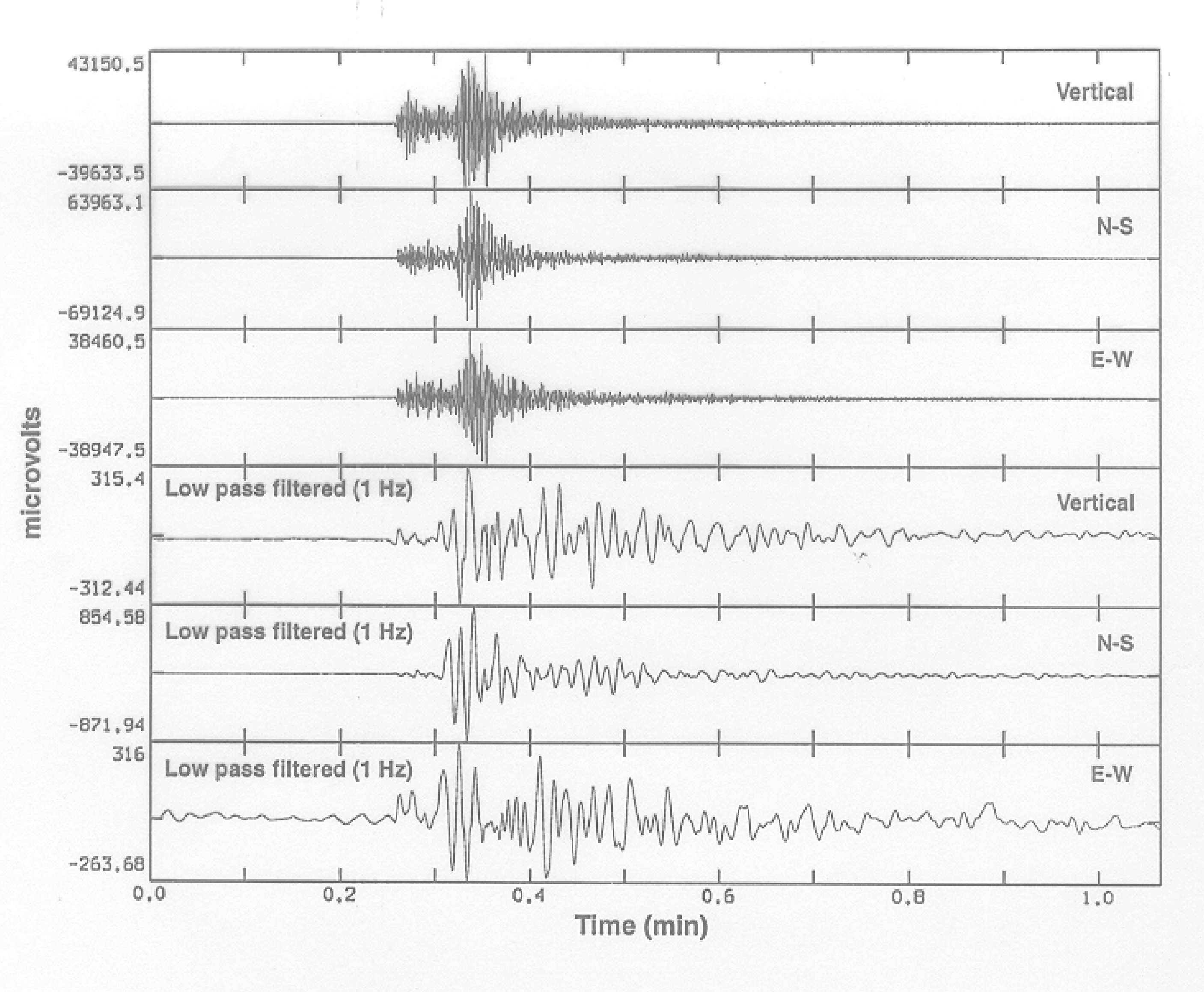

Which portion to invert?

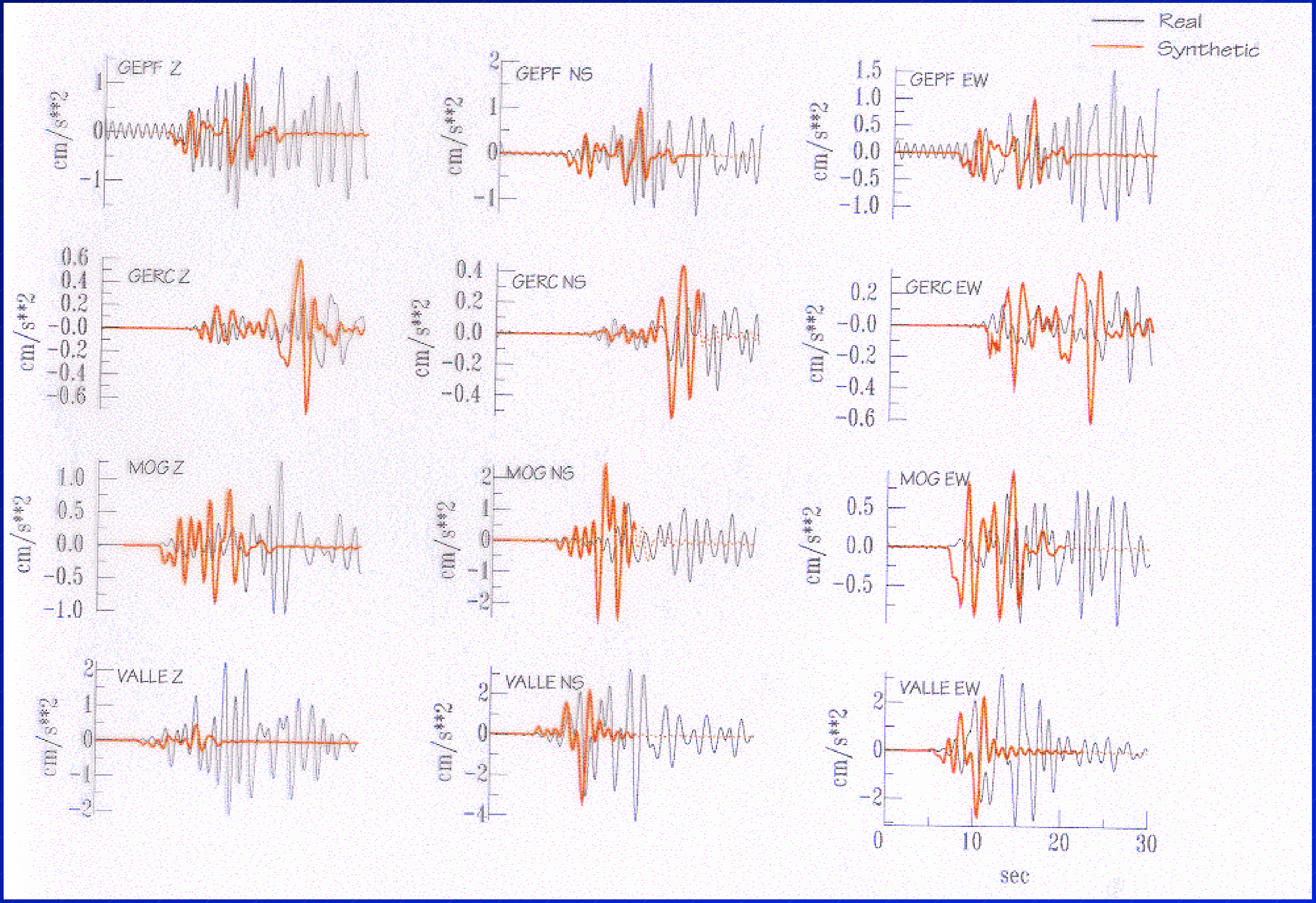

Model 1

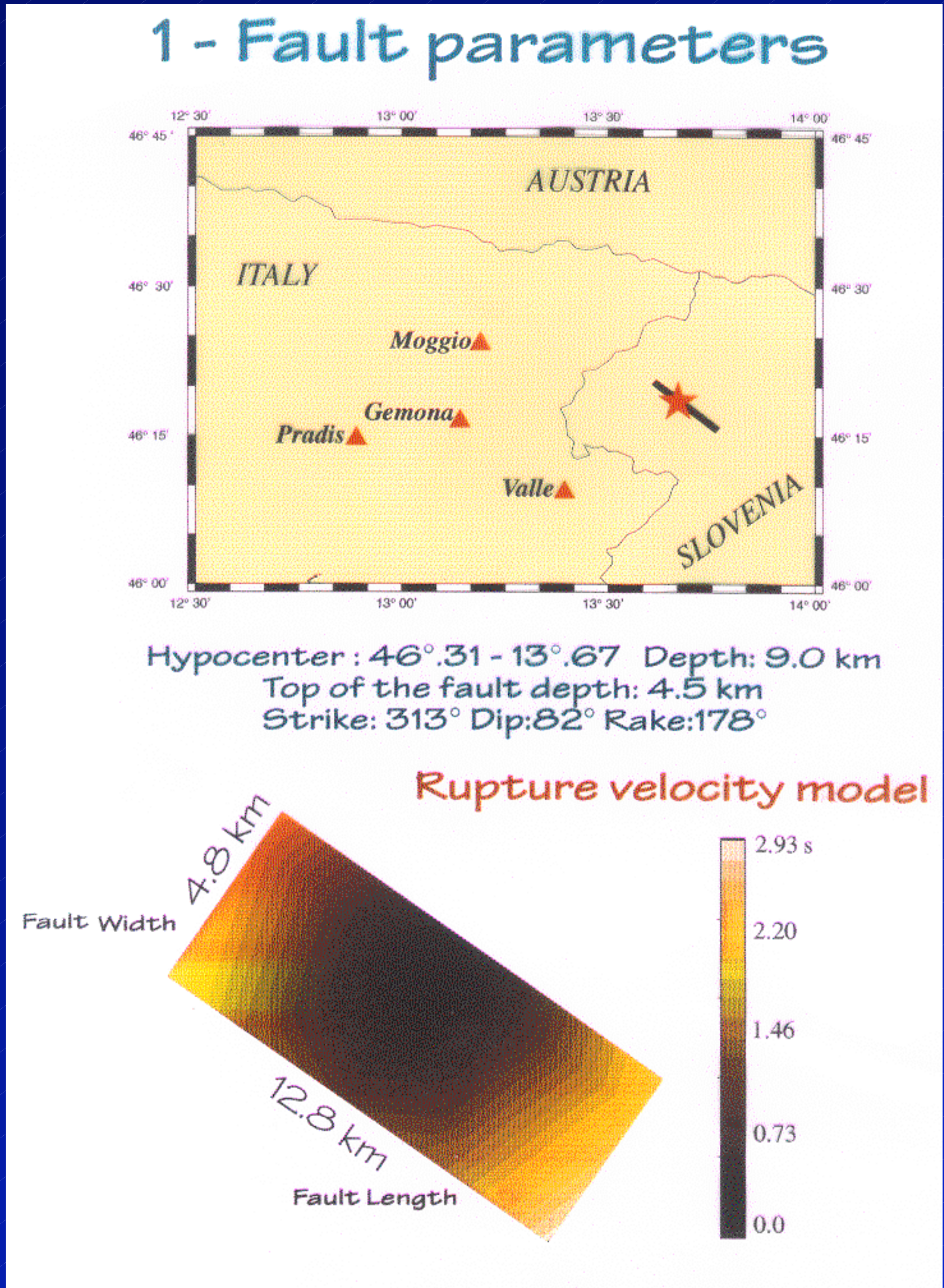

1 - Fault parameters
AUSTRIA
ITALY
SLOVENIA
Moggio
Gemona
Pradis
Valle
12° 30'
13° 00'
13° 30'
14° 00'
46° 45'
46° 30'
46° 15'
46° 00'
Hypocenter : 46°.31 - 13°.67 Depth: 9.0 km
Top of the fault depth: 4.5 km
Strike: 313° Dip:82° Rake:178°
Rupture velocity model
4.8 km
Fault Width
12.8 km
Fault Length
2.93 s
2.20
1.46
0.73
0.0

Model 1

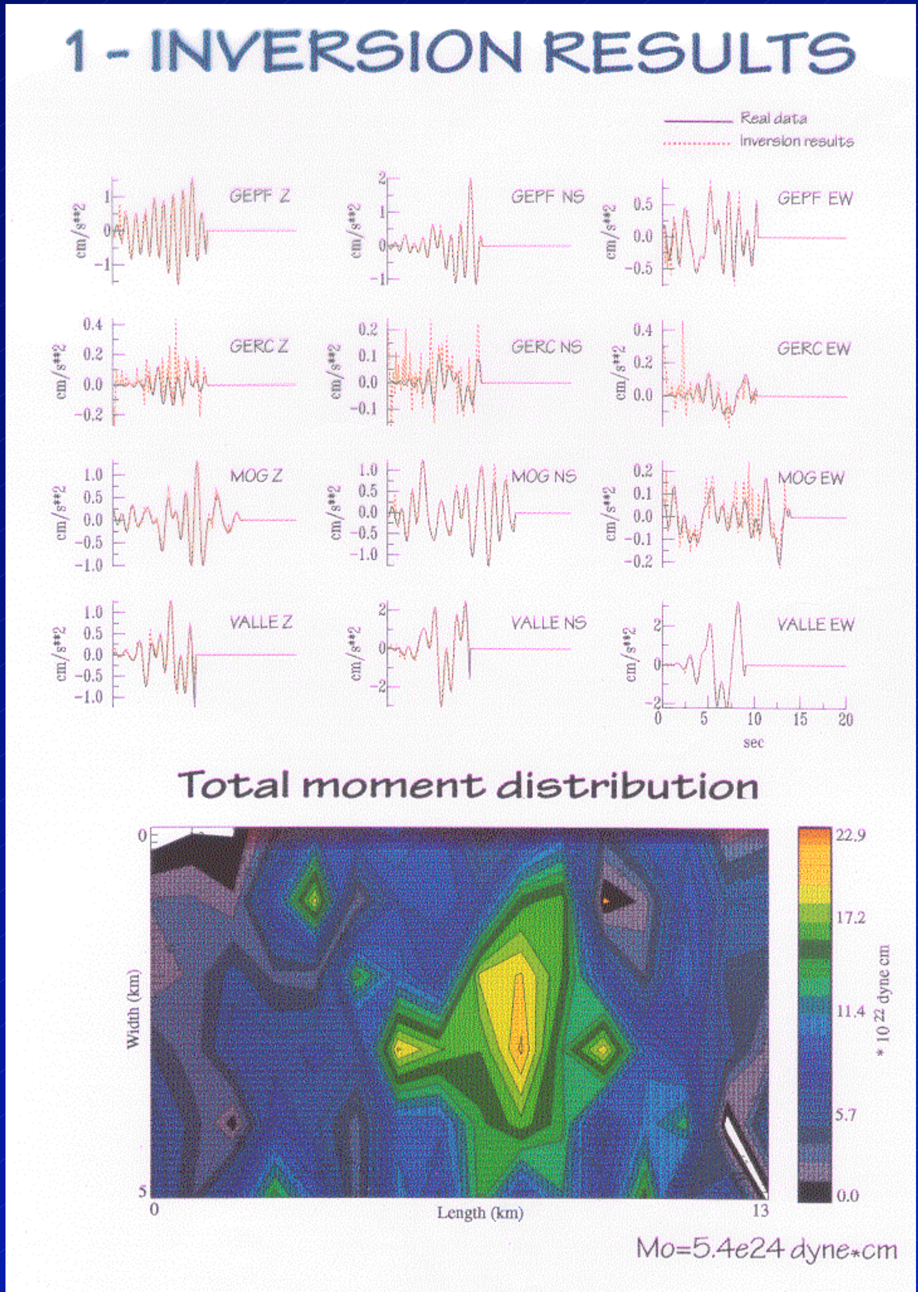
1 - INVERSION RESULTS
Real data
Inversion results
GEPF Z
GEPF NS
GEPF EW
GERC Z
GERC NS
GERC EW
MOG Z
MOG NS
MOG EW
VALLE Z
VALLE NS
VALLE EW
cm/s**2
sec
Total moment distribution
Width (km)
Length (km)
* 10 22 dyne cm
Mo=5.4e24 dyne*cm

Model 2

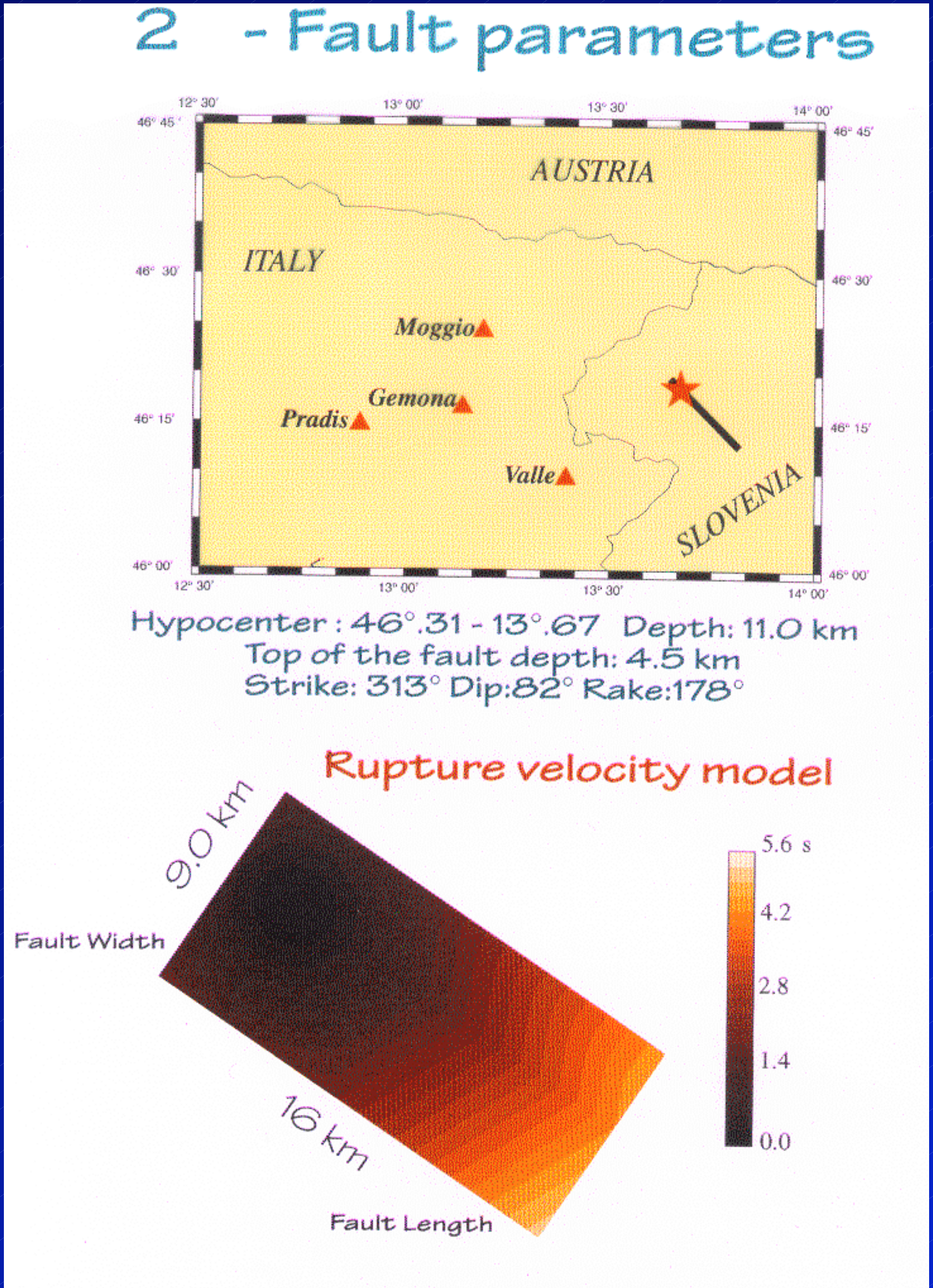
2 - Fault parameters
12° 30'
13° 00'
13° 30'
14° 00'
46° 45'
46° 30'
46° 15'
46° 00'
AUSTRIA
ITALY
Moggio
Gemona
Pradis
Valle
SLOVENIA
Hypocenter : 46°.31 - 13°.67 Depth: 11.0 km
Top of the fault depth: 4.5 km
Strike: 313° Dip:82° Rake:178°
Rupture velocity model
9.0 km
Fault Width
16 km
Fault Length
5.6 s
4.2
2.8
1.4
0.0

Model 2

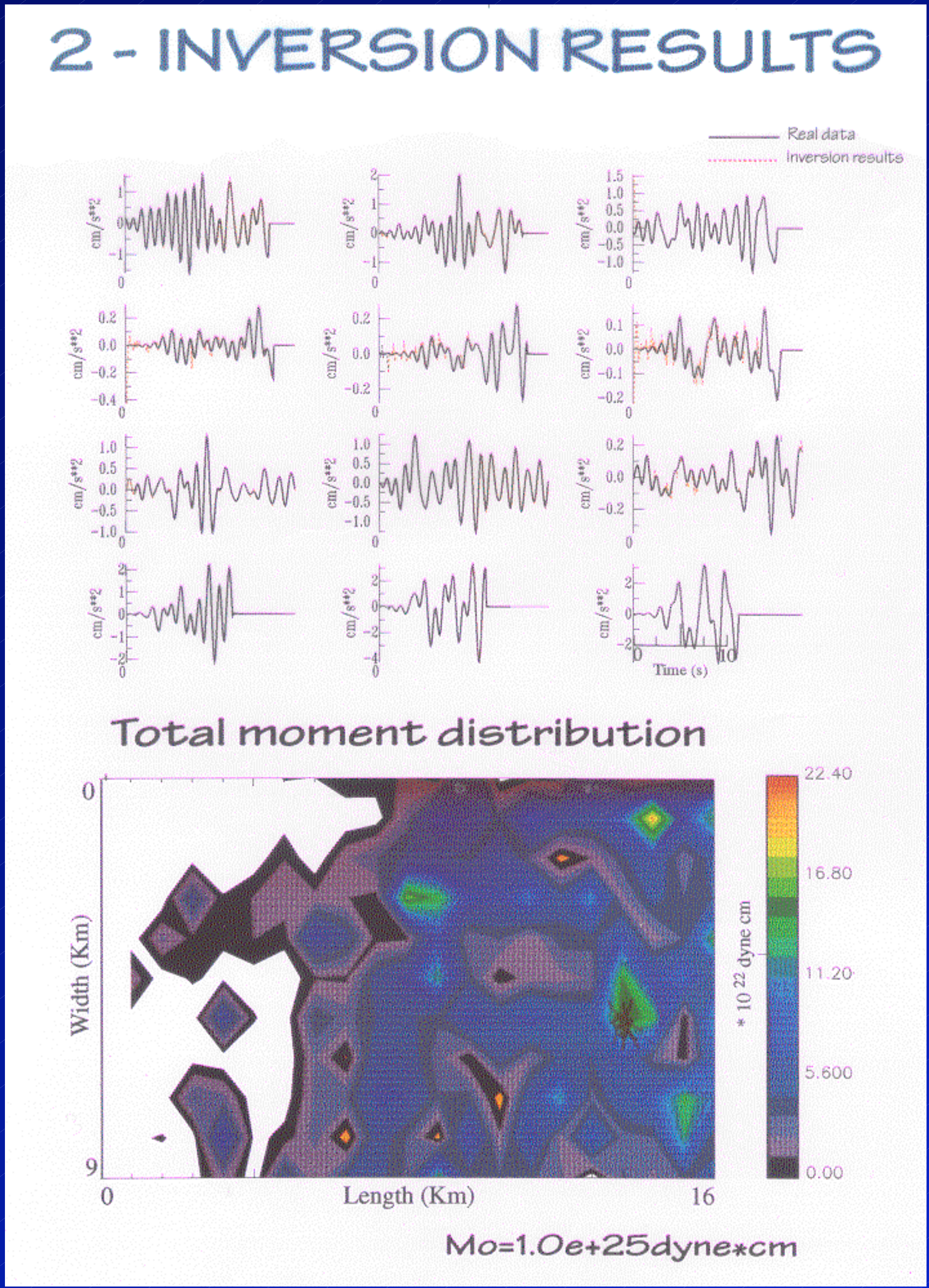

2 - INVERSION RESULTS
Real data
Inversion results
cm/s**2
Time (s)
Total moment distribution
Width (Km)
Length (Km)
* 10 22 dyne cm
22.40
16.80
11.20
5.600
0.00
Mo=1.0e+25dyne*cm

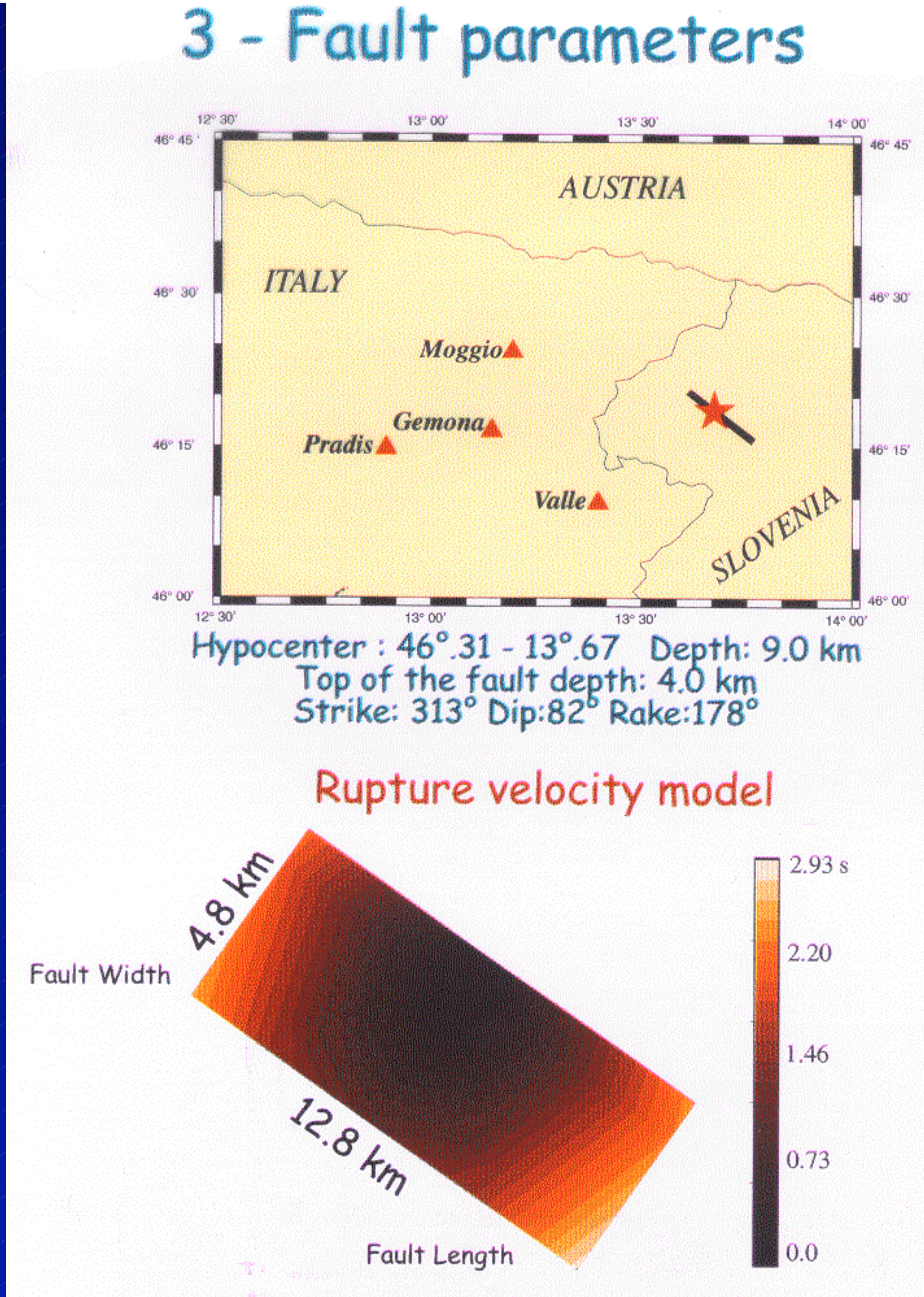
3 - Fault parameters
12° 30'
13° 00'
13° 30'
14° 00'
46° 45'
46° 30'
46° 15'
46° 00'
AUSTRIA
ITALY
Moggio
Gemona
Pradis
Valle
SLOVENIA
Hypocenter : 46°.31 - 13°.67 Depth: 9.0 km
Top of the fault depth: 4.0 km
Strike: 313° Dip:82° Rake:178°
Rupture velocity model
4.8 km
Fault Width
12.8 km
Fault Length
2.93 s
2.20
1.46
0.73
0.0

Model 3

Model 3

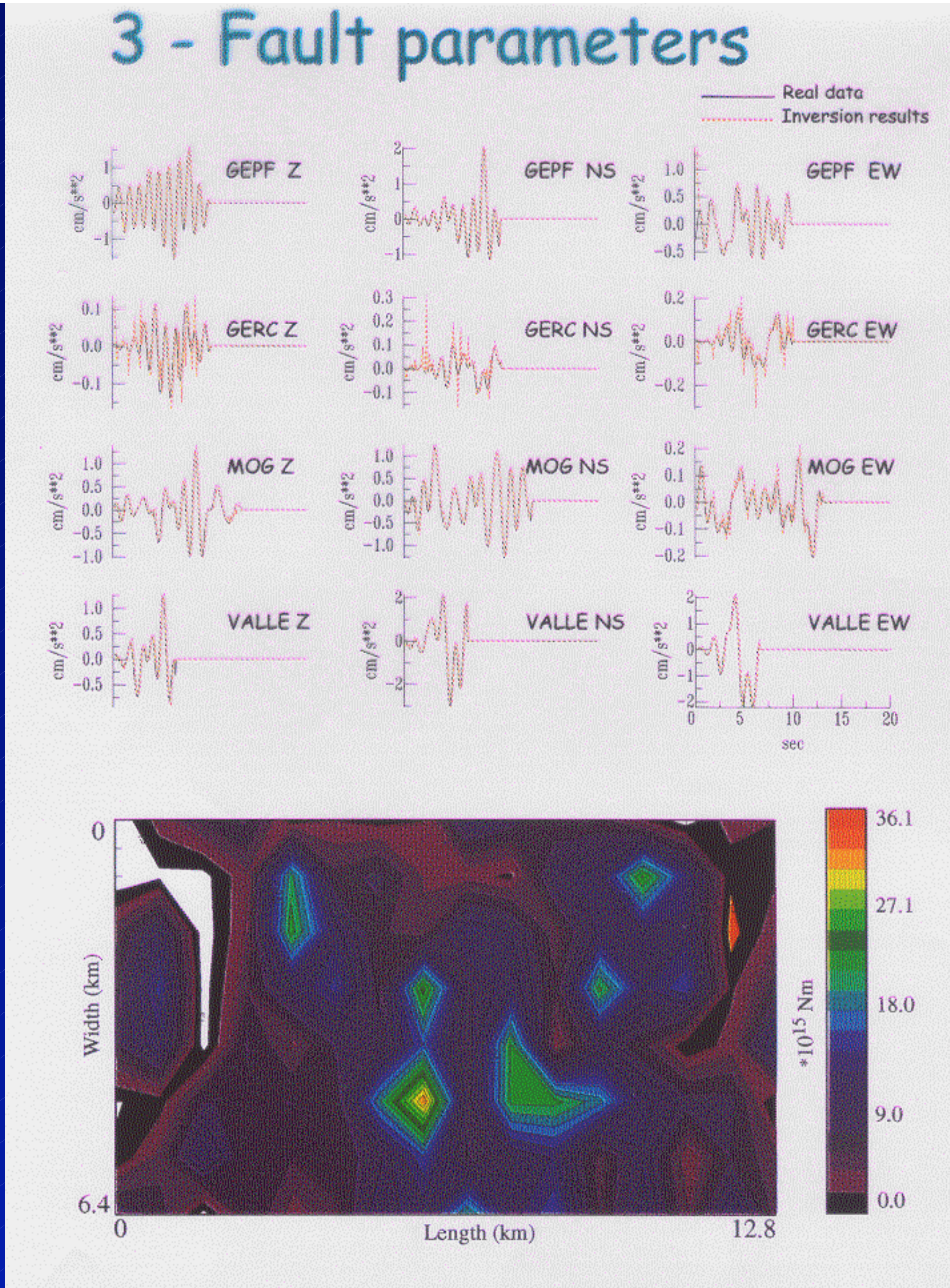
3 - Fault parameters
Real data
Inversion results
GEPF Z
GEPF NS
GEPF EW
GERC Z
GERC NS
GERC EW
MOG Z
MOG NS
MOG EW
VALLE Z
VALLE NS
VALLE EW
cm/s**2
sec
Width (km)
Length (km)
*10^15 Nm
36.1
27.1
18.0
9.0
0.0
6.4
12.8

Results

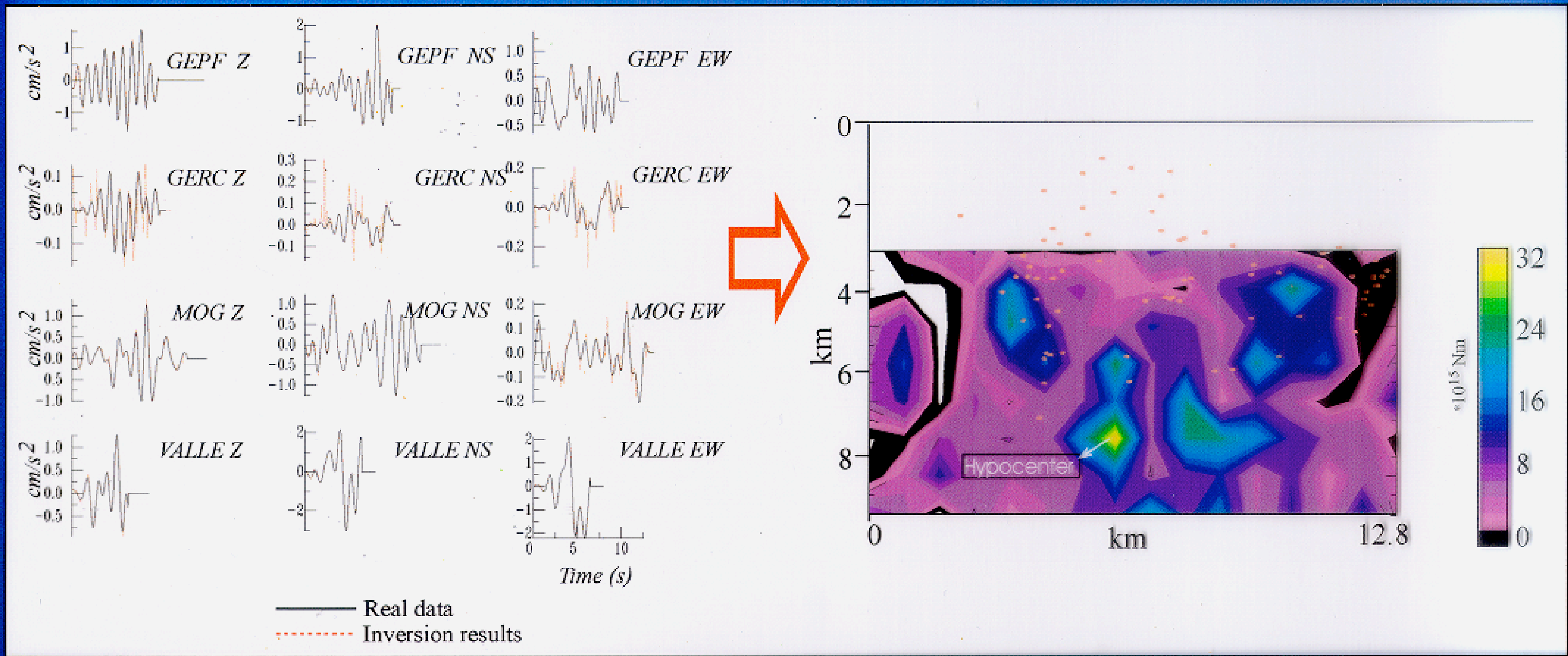

GEPF Z
GEPF NS
GEPF EW
GERC Z
GERC NS
GERC EW
MOG Z
MOG NS
MOG EW
VALLE Z
VALLE NS
VALLE EW
cm/s 2
Time (s)
Real data
Inversion results
km
Hypocenter
0
12.8
*10^15 Nm

Final

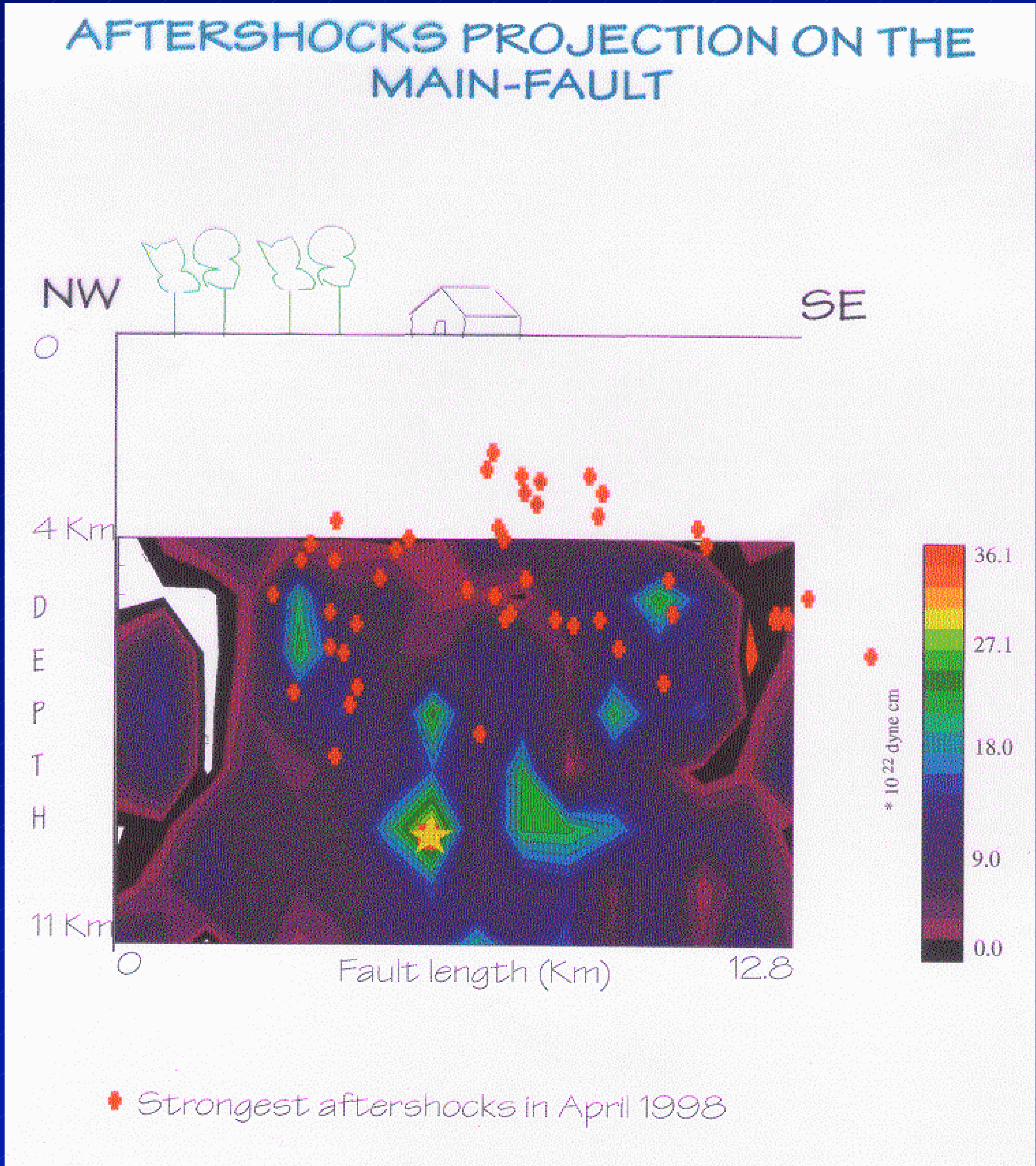

AFTERSHOCKS PROJECTION ON THE MAIN-FAULT
NW
SE
0
4 Km
DEPTH
11 Km
0
Fault length (Km)
12.8
36.1
27.1
18.0
9.0
0.0
* 10 22 dyne cm
Strongest aftershocks in April 1998

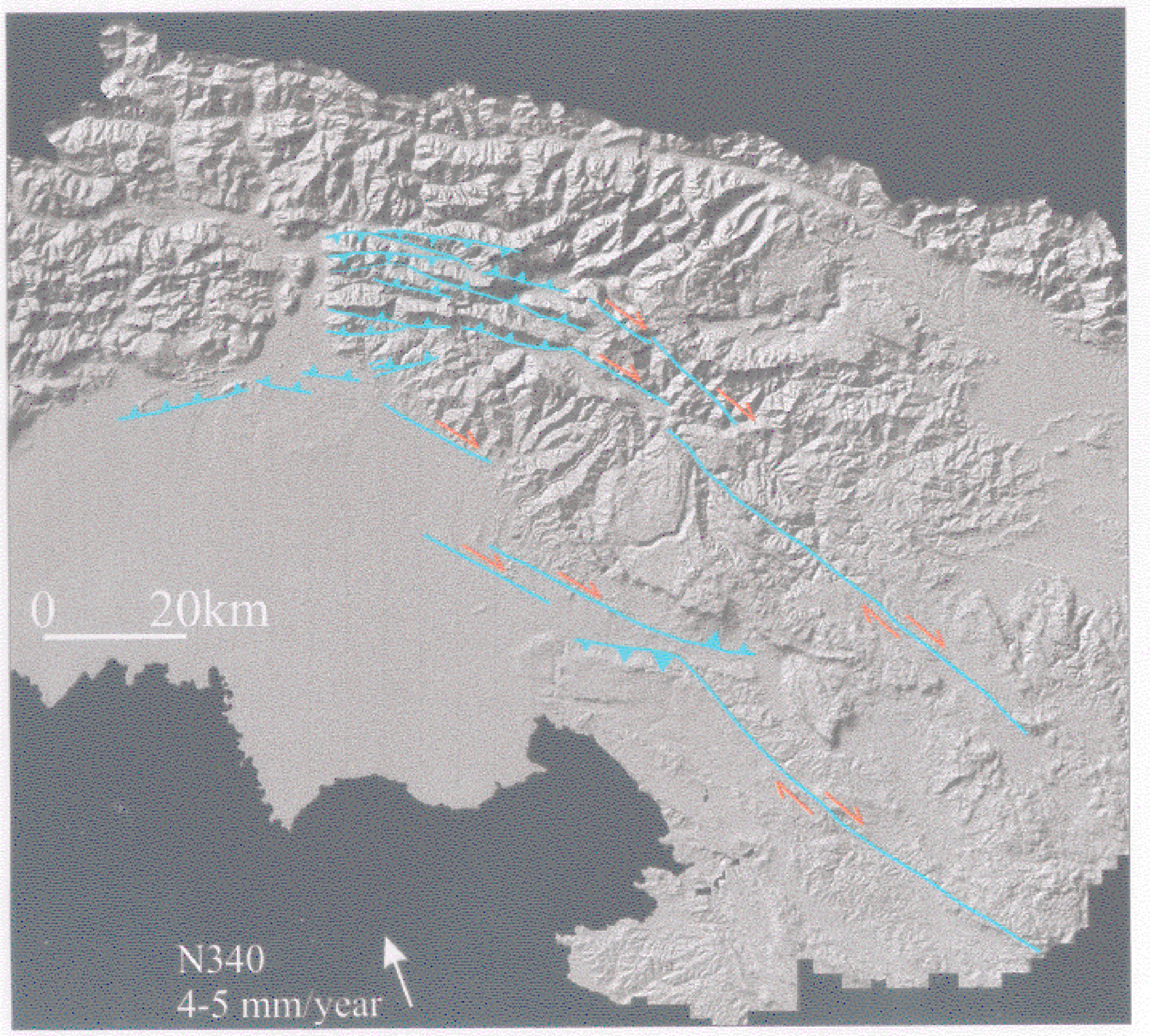

Active faults in NE Italy and W Slovenia

Aoudia(1999)

Slide

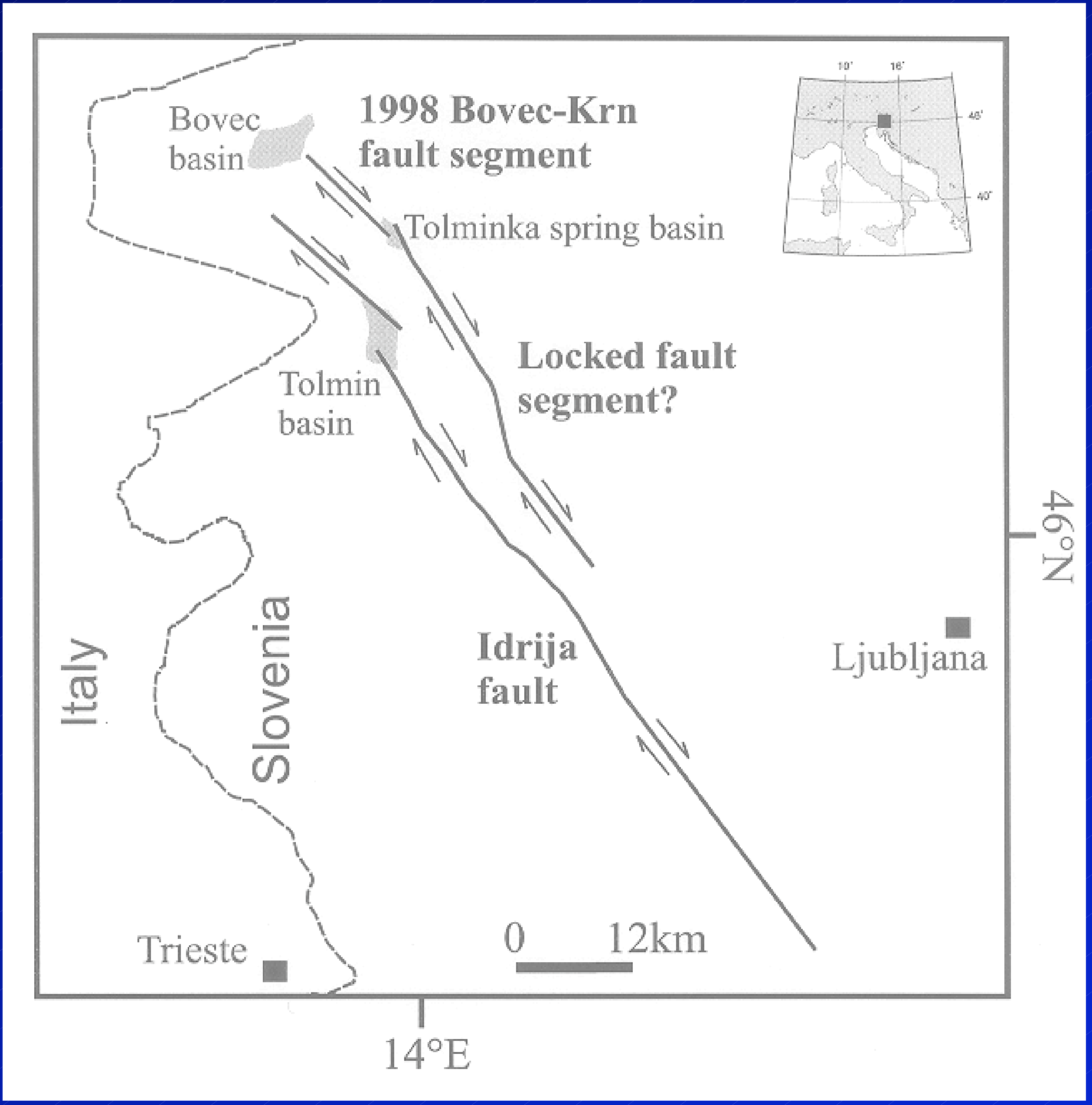

1998 Bovec-Krn fault segment
Bovec basin
Tolminka spring basin
Locked fault segment?
Tolmin basin
Idrija fault
Italy
Slovenia
Ljubljana
Trieste
0 12km
46°N
14°E

The Tolminka Fault

Input Fault Model:

L 35 km, W 10 km,
M 6.6,
θ 320°, δ 80°, λ 176°

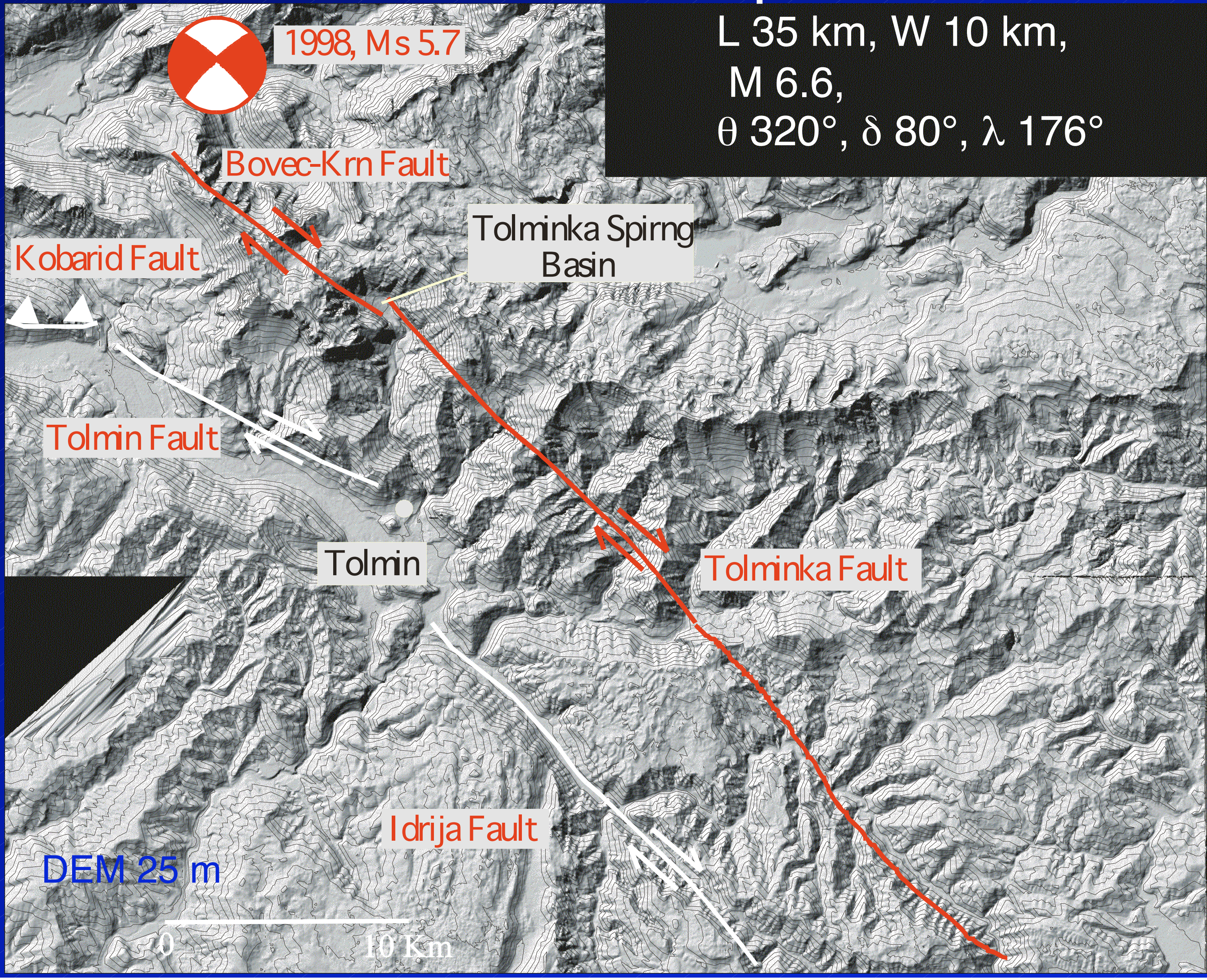

The Tolminka Fault: Results – 1 Hz

Single Asperity

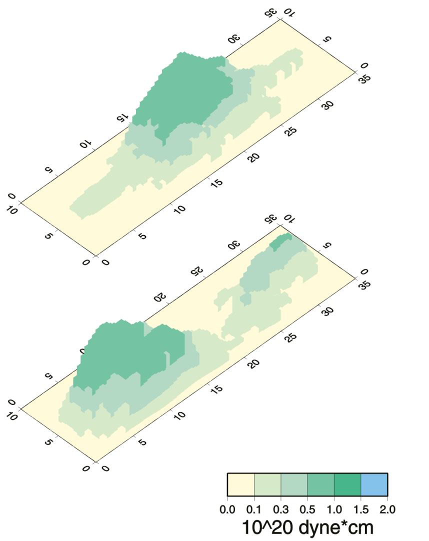

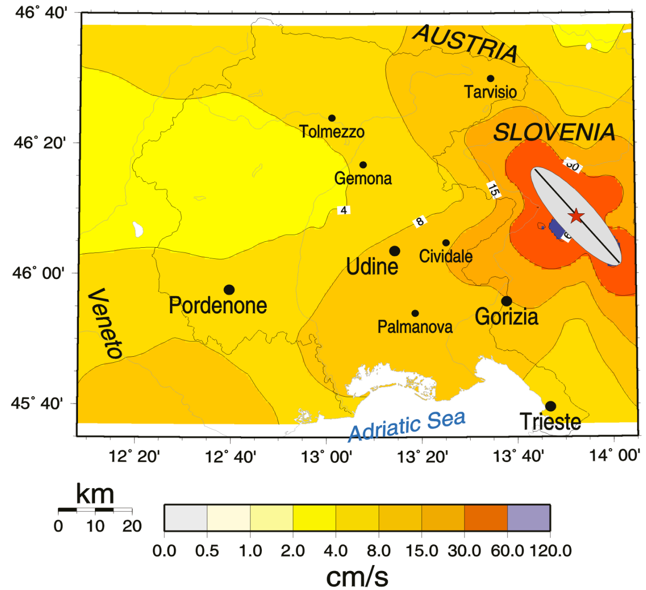

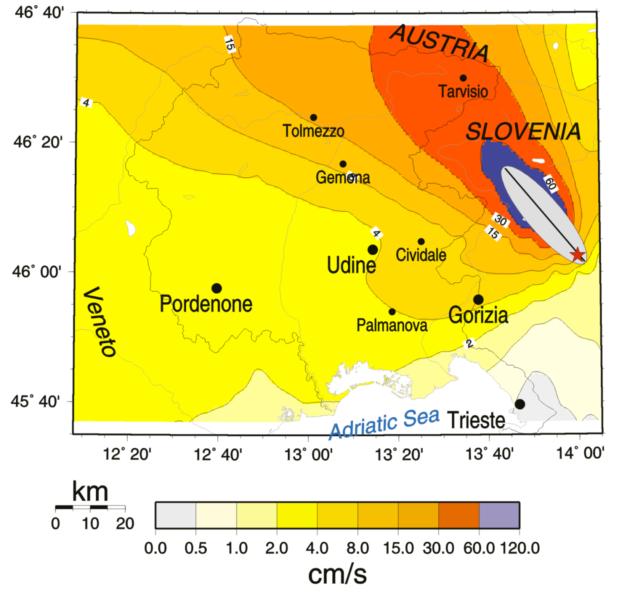

Double Asperity

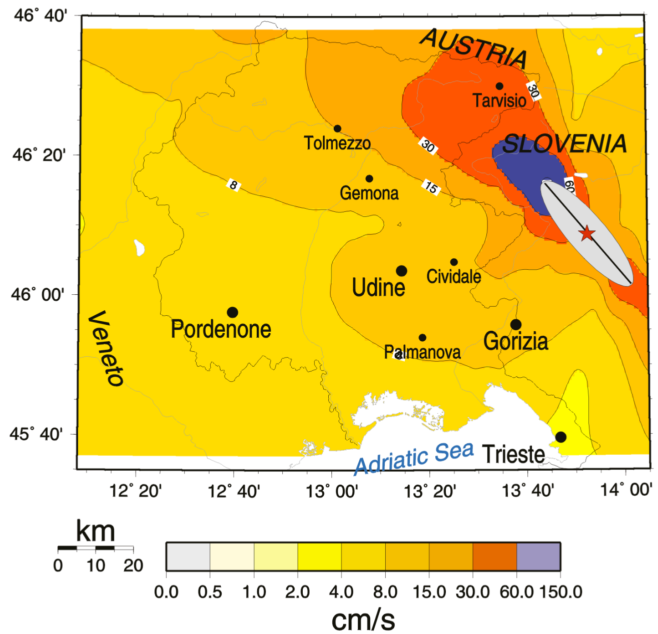

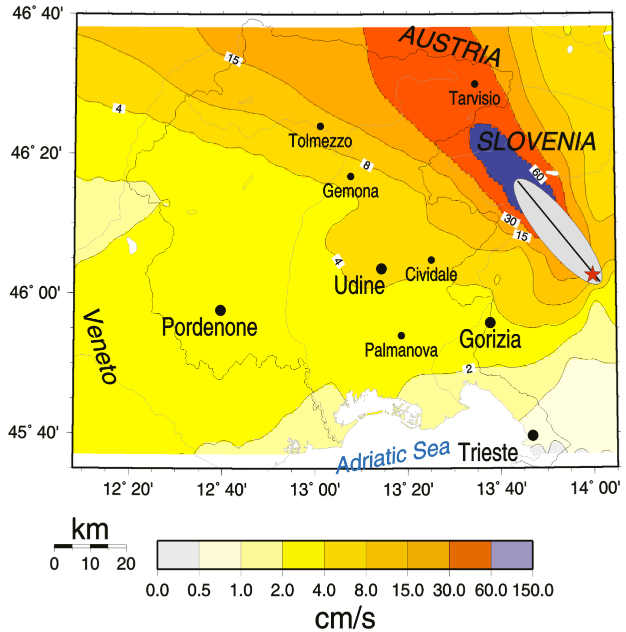

The Kobarid-Tolmin Fault

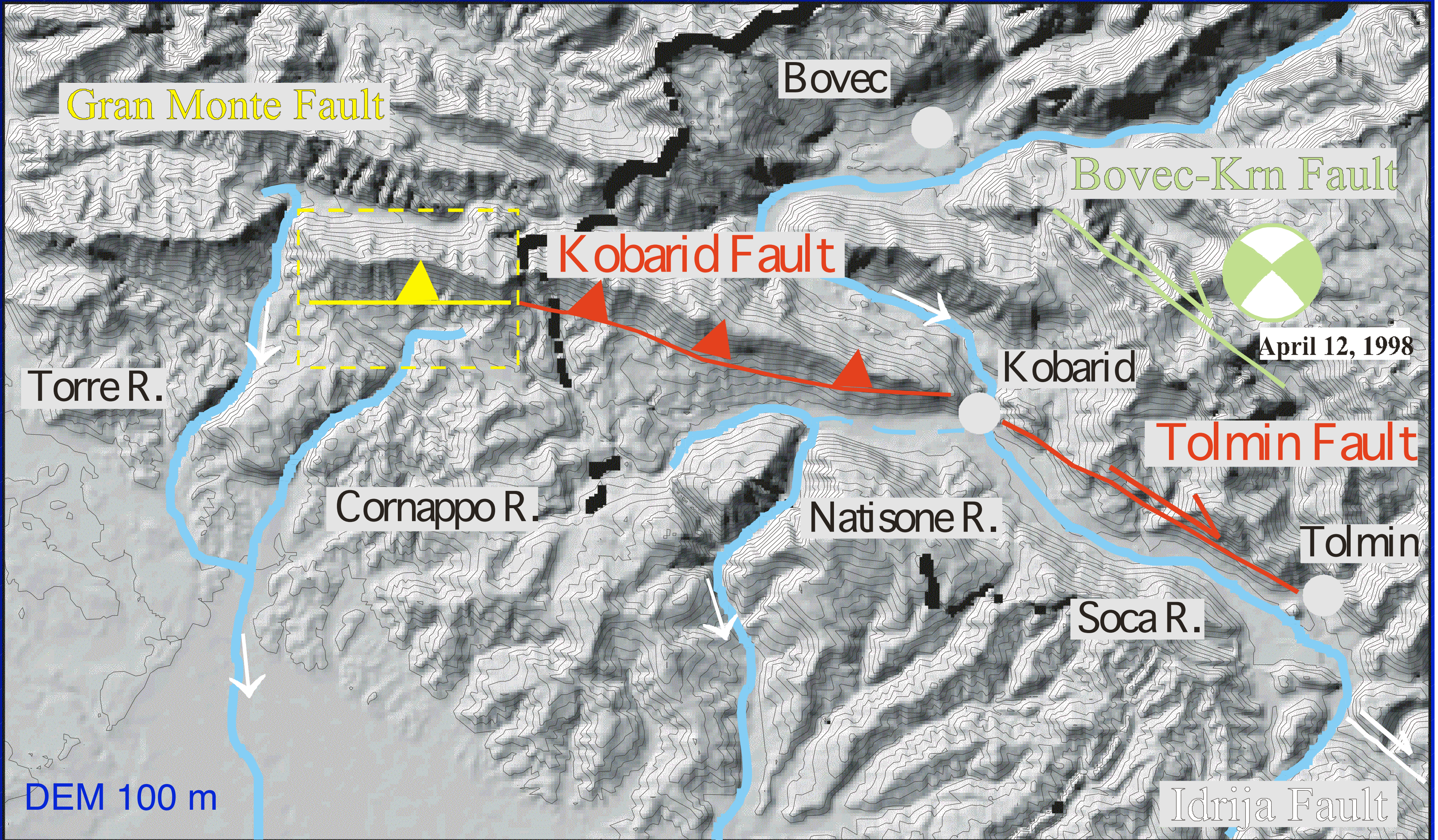

Input Fault Model: L 30 km, W 10.5 km, M 6.6, θ 290°, δ 70°, λ 146°

The Kobarid-Tolmin Fault (1 Hz): Results

Uniform Seismic Moment Distributio

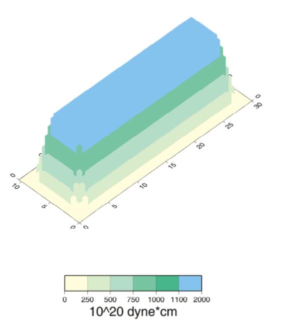

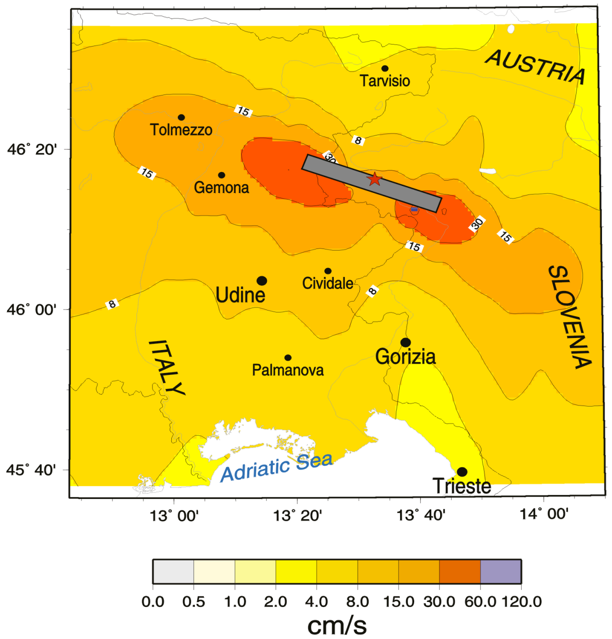

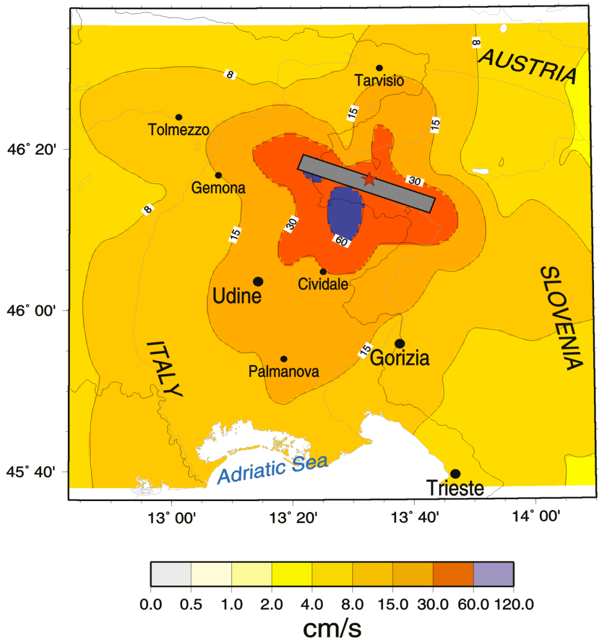

Single Asperity

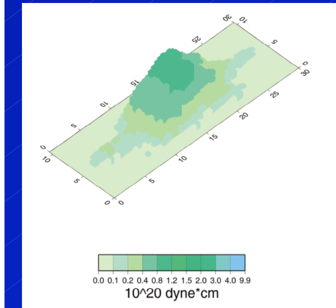

Double Asperity

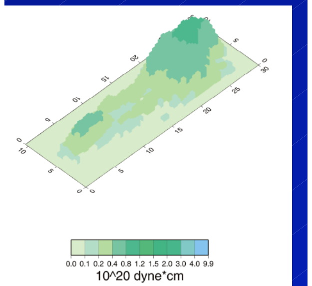

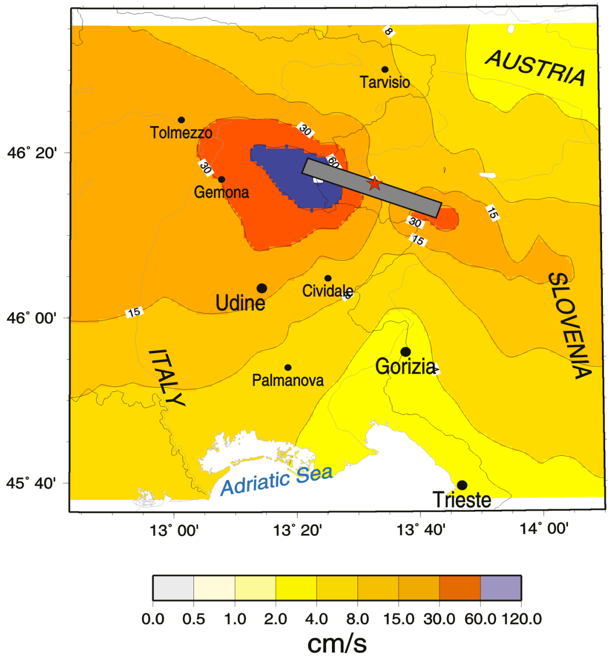

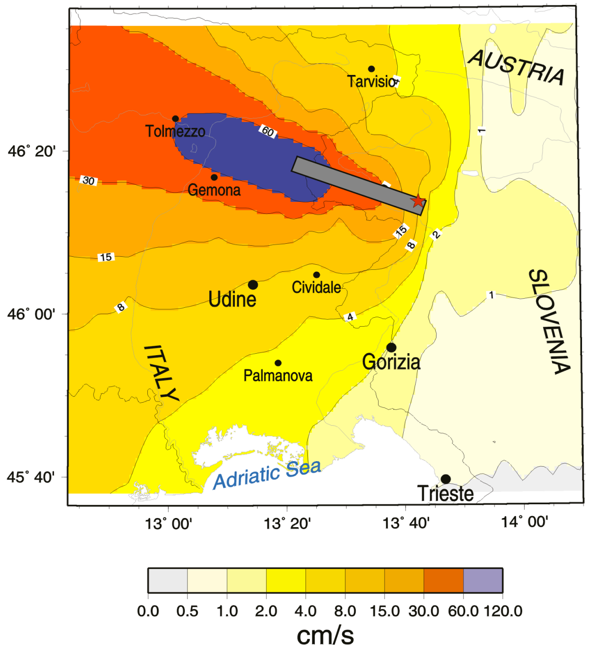

Double Asperity

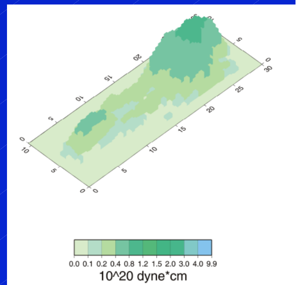

Coulomb stress change

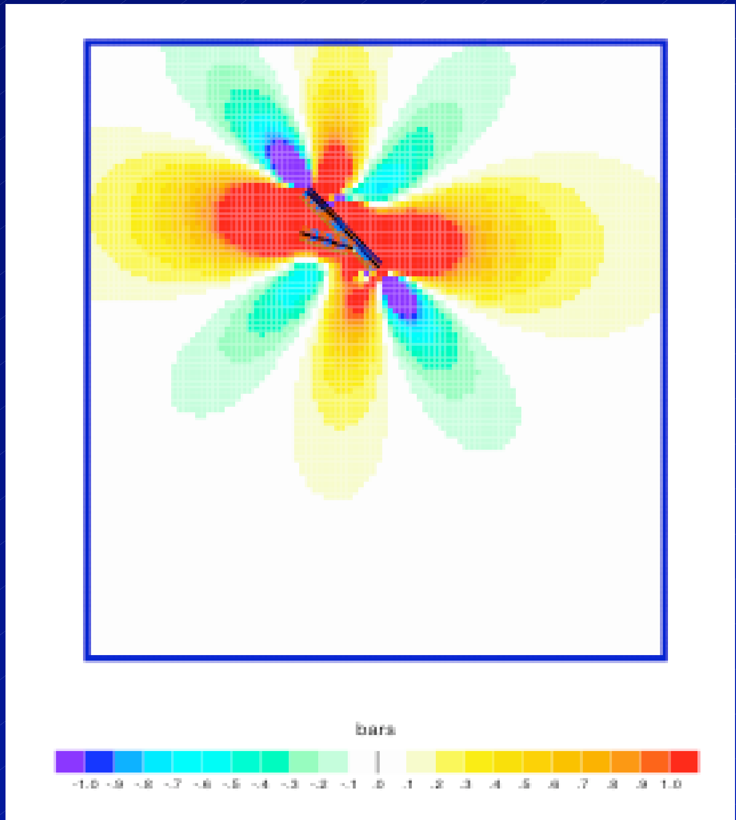

After 1998 event modeled with finite fault model of Bajc et al. (2002)

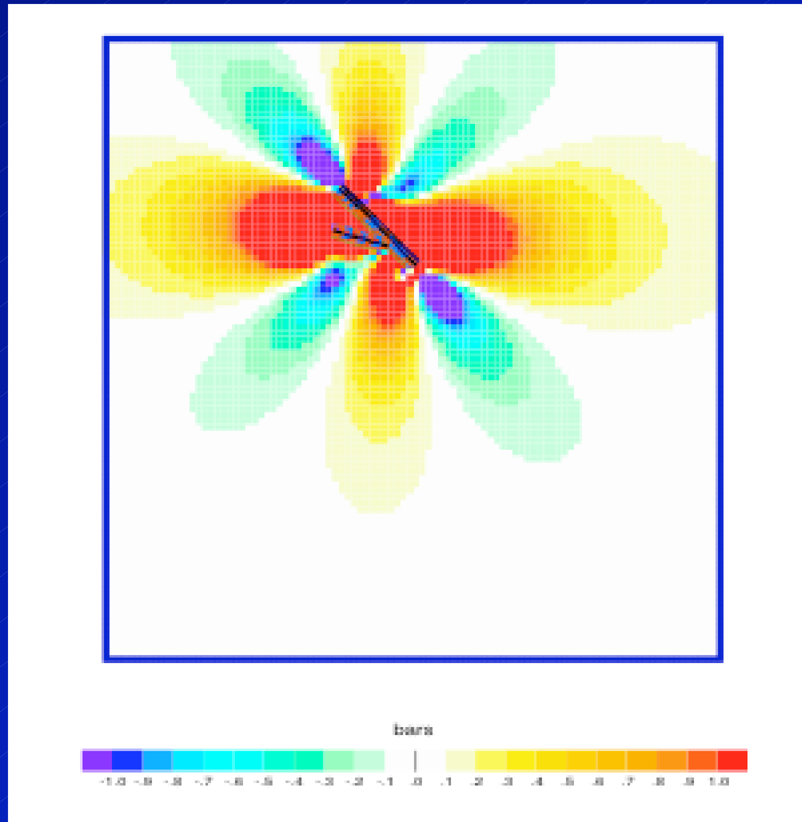

After 1998 and 2004 events: modeled with finite fault models of Bajc et al. (2002) and with uniform slip

Which active fault will rupture next?

The Coulomb stress change would thus favour an increased stress on the Kobarid-Tolmin fault and a reduced stress on the Tolminka fault

Which will be the next ruptured fault depends however on the accumulated stress level on the two faults…